

RESEARCH/REVIEW ARTICLE

Environmental conditions, particle flux and sympagic microalgal succession in spring before the sea-ice break-up in Adélie Land, East Antarctica

Catherine Riaux-Gobin,¹ Gerhard S. Dieckmann,² Michel Poulin,³ Jacques Neveux,⁴ Céline Labruné⁴ & Gilles Vétion⁴

¹ Labex Corail, Joint Research Unit 3278, National Center for Scientific Research, 58 avenue Paul Alduy, FR-66860 Perpignan Cedex, France

² Alfred Wegener Institute for Polar and Marine Research, Am Handelshafen 12, DE-27570 Bremerhaven, Germany

³ Research and Collections, Canadian Museum of Nature, P.O. Box 3443, Station D, Ottawa, Ontario K1P 6P4, Canada

⁴ Laboratoire d'Ecogéochimie des Environnements Benthiques, Research Unit 8222, National Center for Scientific Research and Paris 06 University, FR-66650, Banyuls-sur-Mer, France

Keywords

Land-fast ice; oceanic short-term regime; POM flux; sympagic communities; East Antarctica.

Correspondence

Catherine Riaux-Gobin, Labex Corail, Joint Research Unit 3278, National Center for Scientific Research, 58 avenue Paul Alduy, FR-66860 Perpignan Cedex, France. E-mail: catherine.gobin@univ-perp.fr

Abstract

Data pertaining to environmental conditions, sympagic (sea ice) microalgal dynamics and particle flux were collected before the spring ice break-up 2001 in Pierre Lejay Bay, adjacent to the Dumont d'Urville Station, Petrel Island, East Antarctica. An array of two multiple sediment traps and a current meter was deployed for five weeks, from 8 November to 6 December 2001. The sea-ice chlorophyll *a* and particulate organic carbon (POC) averaged 0.6 mg l^{-1} (30 mg m^{-2}) and 20 mg l^{-1} (1 g m^{-2}) near the coast. The POC export flux that reached a maximum of $79 \text{ mg m}^{-2} \text{ d}^{-1}$ during the study period was high compared to the one for the Weddell Sea. The flux was homogeneous from the surface to 47 m depth and increased sharply 33 days before the effective ice break-up. A north-western progressive vector of currents (i.e., Lagrangian drift) in the sub-ice surface waters was demonstrated. Bottom ice, platelet ice and under-ice water at 5 m were characterized by differences in colonization and short-term succession of microalgae.

Sinking organic material such as protist cells and, more particularly, microalgae to deeper waters in the Southern Ocean and in the seasonal ice zone (SIZ) contributes to the removal of atmospheric CO_2 and provides an important food source for benthic organisms, long before the ice breaks up (Honjo 2004; Fonda Umani et al. 2005). These vertical fluxes have been shown to be highly variable between Antarctic sea-ice regions and can increase significantly after the sea ice retreats (Leventer 2003; Honjo 2004). Several reports have dealt with ice edge algal blooms on the marginal ice zone (MIZ) as an ideal environment for phytoplankton growth (Fonda Umani et al. 2005; Garrity et al. 2005). However, a large part of the Antarctic shelf zone and SIZ still remain poorly investigated due to logistical and technical constraints.

The relationship between particle sinking flux and sea-ice biological productivity has received more attention in the Weddell and Ross seas than along the East Antarctic coast (Leventer 2003). Using predictive models, Garrity et al. (2005) demonstrated a coupling between the sedimentation rate and the ice regime in the Southern Ocean. However, in situ work remains essential for the validation of predictive models, especially in poorly surveyed regions. It is important to quantify the contribution of the sympagic microalgal communities of the bottom ice (Bi) to the overall particle flux, particularly during the sea-ice bloom period and sea-ice melt (Matsuda et al. 1987; McMinn 1996; Günther & Dieckmann 2001; Leventer 2003). Arrigo & Thomas (2004) reported that the Bi algae accounted for up to 25% of the total annual primary production in

ice-covered waters and 1–2 % of the production rate in the Southern Ocean.

Antarctic sea ice reaches its maximum extent in autumn (September–October), roughly 20×10^6 km² (Zwally et al. 1983; McMinn 1996; Comiso 2003), and comprises mainly annual pack ice and drifting pack ice. In coastal regions characterized by colder and less turbulent waters than offshore, land-fast ice develops without noticeable contribution of frazil ice (Arrigo & Thomas 2004). The annual first-year ice consists of columnar ice composed of vertically elongated crystals and a biologically productive bottom layer often composed of granular ice (McMinn et al. 2007). The Bi horizon is steadily colonized by sympagic communities, which are similar in taxonomic composition across coastal Antarctic circumpolar regions (Palmisano & Garrison 1993; Günther & Dieckmann 2001). They are mainly composed of colonial and solitary diatoms (Watanabe et al. 1990) and various other one-celled eukaryotes (Scott & Marchand 2005). The platelet ice layer (Pi), which is commonly associated with land-fast ice, is particularly enhanced in the proximity and by the extent of ice shelves (Foldvik & Kvinge 1977; Dieckmann et al. 1986; Arrigo et al. 1995; Leonard et al. 2006). Detailed investigations around Antarctica during the last decade confirmed the occurrence of highly productive communities in the Pi horizon (Arrigo et al. 1995; Robinson et al. 1998; Günther et al. 1999; Thomas et al. 2001).

In pack ice, the microalgal biomass is distributed throughout the ice matrix in different layers, such as the subsurface infiltration layer and internal or intermediary layers (Garrison & Buck 1989; McMinn et al. 2000). As a result, the under-ice particle flux from the pack ice has been shown to extend over a long period of time (Leventer & Dunbar 1987; Leventer 2003). In contrast, the spring microalgal biomass in Antarctic land-fast ice is usually concentrated in a relatively constrained layer and the sedimentation process has been shown to be linked to the first melting events (Leventer 2003). In Lützw-Holm Bay, near Syowa Station, the annual sedimentation under the fast ice was shown to be depleted in winter, starting again in November, and reaching a maximum particulate organic carbon (POC) export flux of $140 \text{ mg m}^{-2} \text{ d}^{-1}$, in February–March (Matsuda et al. 1987).

The sympagic communities off Adélie Land in East Antarctica has received some consideration during the past decade (Delille et al. 2002; Riaux-Gobin & Poulin 2004; Riaux-Gobin et al. 2005; Fiala et al. 2006; Poulin et al. 2006; Riaux-Gobin et al. 2011). Formed annually, the land-fast ice is less than 1.5 m thick in Pierre Lejay Bay (Riaux-Gobin et al. 2005; Riaux-Gobin et al. 2011). The sympagic community is present in April and May

until the ice break-up in December or January (Riaux-Gobin et al. 2000; Riaux-Gobin et al. 2005; Fiala et al. 2006), and it is restricted in springtime to a thin layer (often less than 5 cm) at the proximate part of the Bi (Riaux-Gobin et al. 2005). A Pi layer (see below) is always present under the Bi and shows differences in colonization from year to year (Riaux-Gobin et al. 2005).

In land-fast ice off Adélie Land, the microalgal biomass is largely dominant over the bacterial and protozoan components (Fiala et al. 2006). The sympagic community shows high summer Chl *a* concentrations up to 1.9 g m^{-2} in 1995 (Riaux-Gobin et al. 2000), but with a relatively low number of diatom taxa (<40 and 53 in 1995 and 2001, respectively), and the dominance of a low number of taxa (Riaux-Gobin et al. 2003). A thin Pi layer <40 cm thick forms from year to year off Adélie Land (Riaux-Gobin et al. 2003). This Pi layer is clearly distinct from the Bi and in springtime consists of a loose matrix of intertwined ice crystals with a sherbet-like consistency. The colonization of Pi is different from that of the Bi in annually formed sea ice at Terra Nova Bay, Ross Sea (Guglielmo et al. 2004). Some differences in the distribution of the most dominant species between the Bi and Pi habitats have been reported in Adélie Land by Riaux-Gobin et al. (2003). The chemistry of the Adélie Land Pi also suggests a different origin for Bi and Pi (Riaux-Gobin et al. 2000; Riaux-Gobin et al. 2005; this study). This hypothesis is supported by the fact that the Astrolabe Glacier, located about 2.4 km from our sampling station (Fig. 1), influences environmental conditions (i.e., low temperatures) close to the sampling site. However, in contrast to the Weddell Sea (Thomas et al. 2001), the small thickness of Pi in Adélie Land may cause an intensification of the particulate organic matter (POM) and nutrient fluxes towards the underlying surface waters.

The main objectives of this study were: (1) to quantify the sub-ice POM sinking export to deeper waters before the spring ice break-up in Pierre Lejay Bay; (2) to characterize the species succession in Bi and Pi sympagic communities prior to the ice break-up during the austral spring 2001/02 off Adélie Land; and (3) to briefly explain the hydrological and meteorological data accompanying these observations.

Sampling site, material and methods

Site, environmental data and measurements

The sampling programme was conducted at a fixed station R1 ($66^{\circ} 39.223'S$, $140^{\circ} 00.139'E$; Fig. 1) at a water depth of 53 m, ca. 300 m off the Dumont d'Urville Station on Petrel Island (Île des Pétrils) in East Antarctica, from

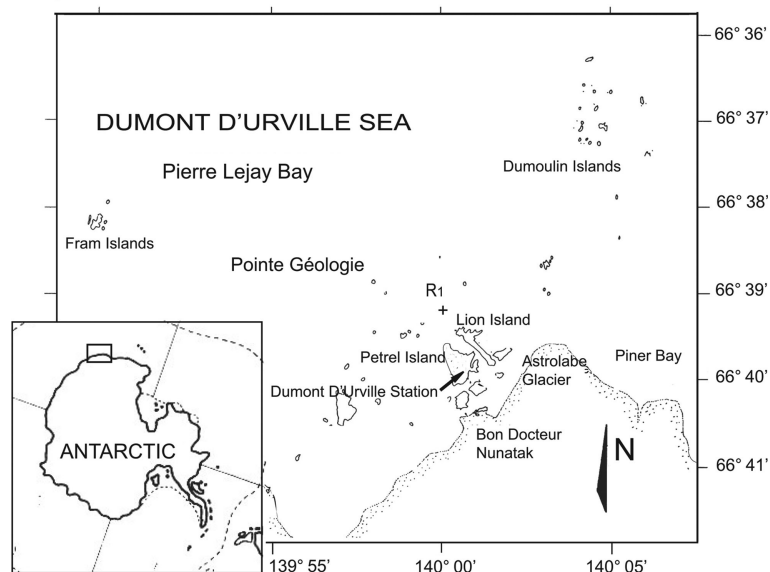


Fig. 1 Map showing the position of station R1 (+) in Pierre Lejay Bay, Dumont d'Urville Sea, Adélie Land, East Antarctica.

1 November (day 1) to 29 December 2001 (day 59). The station R1 was the same one visited in previous expeditions (Riaux-Gobin et al. 2000; Riaux-Gobin et al. 2003; Riaux-Gobin et al. 2005). The ice conditions and structure were the same as described by Riaux-Gobin et al. (2003), with the ice break-up occurring on 10 January 2002 in this study. Discrete daily sampling was performed on the Bi, Pi and under-ice water at 5 m (UIW5).

Infrared satellite images (Fig. 2) and meteorological data (Fig. 3) were provided by the Dumont d'Urville meteorological station (Météo France and MétéoSat). The satellite images were obtained from NOAA12 and NOAA14 satellites, equipped with an advanced very high-resolution radiometer with five channels and 1-km vertical resolution and 4-km lateral resolution. After computer-aided processing provided by the Service d'Archivage et de Traitement Météorologique des Observations Satellitaires, in Lannion, France, the composite images were used to distinguish ice, water and cloud cover. The continental boundary is taken from map 6061, provided by the Service Hydrographique et Océanographique de la Marine. The limits of the glacier tongues—particularly the highly variable Dibble Tongue are artificially included as “continental limits” (Fig. 2). The day length measured by a heliograph with fibre optics at the meteorological station at Dumont d'Urville Station (Fig. 1) is defined as the time during which the light level was $> 120 \text{ W m}^{-2}$ (Fig. 3). The theoretical tidal data (Fig. 3) were obtained from the French Naval Hydrographic and Oceanographic Service (Pineau 1999; Le Roy & Simon 2003) and the Sub-

antarctic and Antarctic Sea level Observation Network, established by the Laboratory for Studies in Geophysics and Spatial Oceanography in Toulouse.

Two multiple MST-6 sediment traps (Hydro-Bios, Kiel, Germany) were deployed under the land-fast ice at R1 for five weeks from 8 November to 6 December (Fig. 4). Each trap had an opening area 0.015 m^2 , covered by a 40-mm thick plastic grid, with 40 mm^2 holes. Each trap was equipped with six 250-ml sample cups, filled with filtered seawater poisoned with 1% HgCl_2 that rotated at a pre-set interval of six days. The top trap was located at 3 m under the land-fast ice, with an RCM7 current meter (Aanderaa Data Instruments, Nesttun, Norway) directly underneath it, while the bottom trap was positioned at 6 m above the seafloor (Fig. 3). The whole array system was stabilized with a mooring anchor. After the recovery of the sediment traps, the sample cups were split into sub-samples for later determinations of POC, nitrogen (PON) and chloropigments. The current meter, which was equipped with a temperature sensor, was programmed to register data every 20 min. The progressive diagram of currents was calculated with Aanderaa software.

Sub-ice salinity and temperature profiles (0–50 m) were obtained from 3 November to 14 December using an SBE 37-SI MicroCAT conductivity–temperature profiler equipped with an SBE ST pump (Sea-Bird Electronics, Bellevue, WA, USA). The instrument had a resolution of 0.0001°C and 0.0001 psu and was calibrated by Sea-Bird Electronics prior to and after use. Daily profiles were always taken at noon.

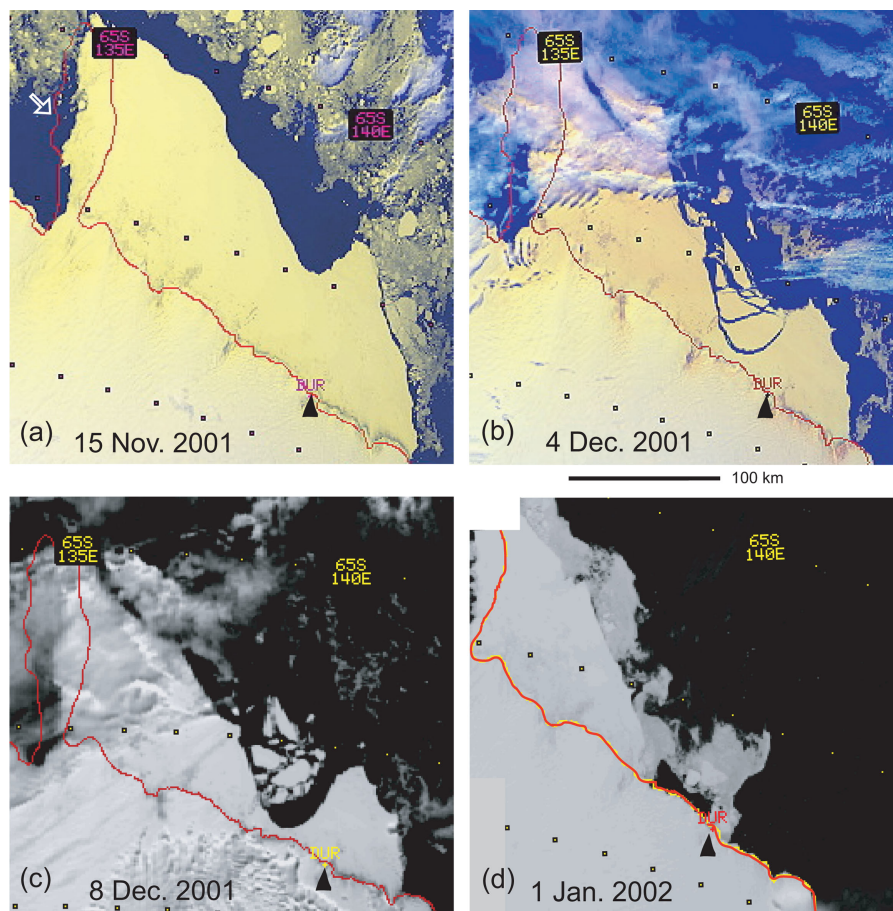


Fig. 2 MétéoSat infra-red satellite images of the sea-ice extent and changes during the ice break-up, Adélie Land, Antarctica from 15 November 2001 to 1 January 2002 (from NOAA12 and NOAA14, via the Service d'Archivage et de Traitement Météorologique des Observations Satellitaires, Lannion, France). The black arrows show station R1 in the Dumont d'Urville Sea and the white arrow in (a) shows the Dibble Glacier tongue. The red lines demarcate the continental limits for the purposes of this study.

During the 59-day sampling programme, a total of 19 discrete samplings of Bi, Pi and underlying water at 5 m water depth (UIW5) were acquired from 1 November (day 1) to 29 December (day 59) within a reduced surface ($<60 \text{ m}^2$) to minimize the impact of spatial heterogeneity/patchiness (see Discussion section).

On each sampling day, snow and ice thickness and sub-ice irradiance were measured at noon local time. The instrument used was an SA light sensor (Li-COR Biosciences, Lincoln, NE, USA), equipped with a Spherical Quantum Sensor LI-193SB, operating through the ice coring hole (around 8 cm in diameter), which was covered by a lid. The resulting 0–40 m profiles give a rough estimate of the light reaching the sympagic algal layer at the base of the ice column.

Two to three ice cores were collected during each visit with a SIPRE coring auger (i.e., of the type developed by the US Army Snow, Ice and Permafrost Research

Establishment) with an inner diameter of 7.5 cm. Each core was stored separately in a black plastic bag and kept at -20°C at the Dumont d'Urville Station where the last 5 cm of the Bi was removed with a stainless steel saw. The sherbet-like Pi was rapidly scooped out from the core hole with a stainless steel ladle, stored in plastic or glass containers and kept at -20°C . As a rough indication, the Pi thickness was evaluated when scooped. Ice core samples were slowly melted in the dark at $4-7^\circ\text{C}$ from a few hours for Pi samples to 12–16 h for Bi samples. Water samples were collected at 5 m depth (UIW5) with a simple hydrological bottle consisting of a weighted polyethylene cylinder with a stopper operating from the surface (Riaux-Gobin et al. 2003).

Analytical methods

Physical and chemical variables. The salinity and pH of UIW5 samples and meltwater Bi and Pi samples

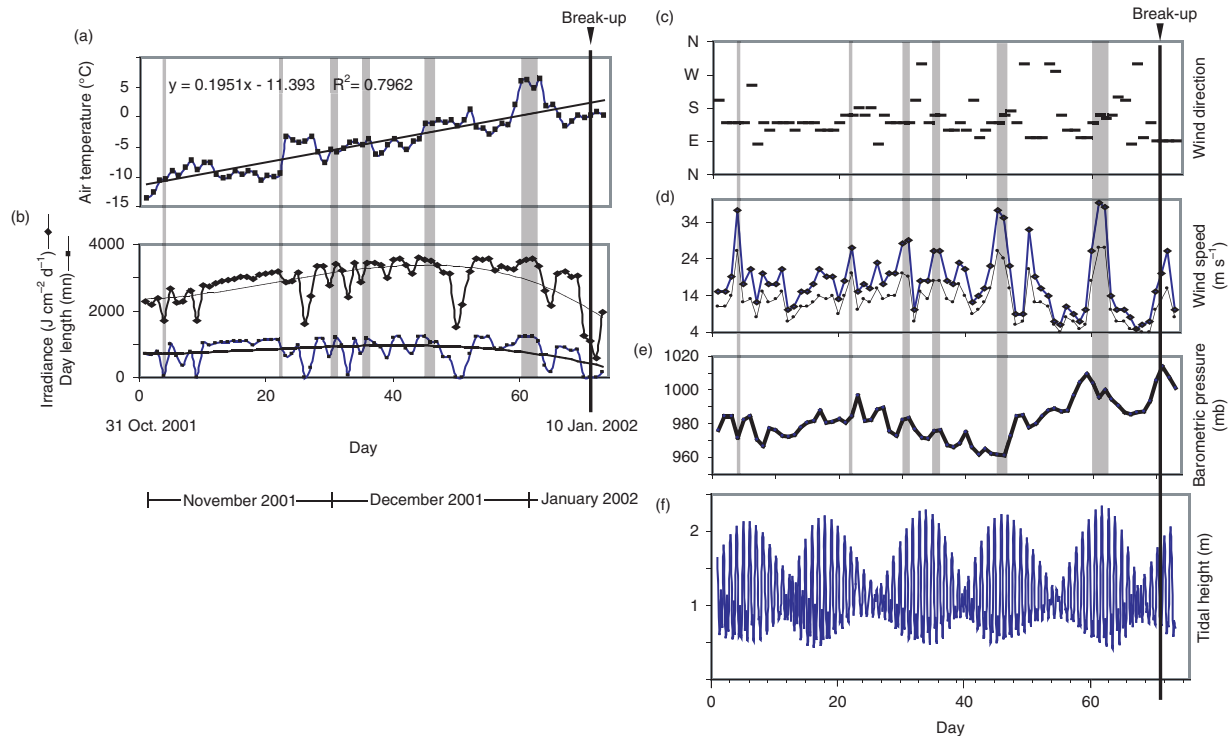


Fig. 3 Temporal variations of (a) air temperature, (b) surface irradiance, (c) wind direction, (d) wind speed, (e) air pressure and (f) tidal height data at the Dumont d'Urville Station from 1 November 2001 to 12 January 2002. Shaded areas indicate the strongest katabatic wind events.

were measured with a conductivity and pH meter (SP536; psu: +0.5; pH: +0.02). For pigment analysis, water samples were filtered on 47-mm GF/F filters (Whatman, Kent, UK) and kept frozen at $-20^{\circ}C$ for later analyses at the Banyuls-sur-Mer Biological Oceanography Laboratory. After a 100% acetone extraction in the dark at $4-7^{\circ}C$, following procedures described by Neveux & Lantoine (1993), the concentrations of Chl *a*, *b* and *c* and breakdown phaeopigments (Phaeo) *a*, *b* and *c* were determined with an LS 55 Fluorescence Spectrometer (Perkin Elmer, Waltham, MA, USA), using Perkin Elmer's FL WinLab software. The results for Chl *b*, Phaeo *b* and Phaeo *c* are not presented since these concentrations were negligible in sea ice, although noticeable Chl *b* concentrations were observed in open water after the ice break-up (Riaux-Gobin et al. 2011).

Bi, Pi and UIW5 water samples for nutrient (nitrate + nitrite: $NO_3^- + NO_2^-$, nitrite, phosphate: PO_4^- and silicic acid: $Si[OH]_4$) measurements were filtered on a 50- μm sieve to eliminate clumps of microalgae and meiofauna and immediately frozen at $-20^{\circ}C$ for later analyses at the Banyuls-sur-Mer Biological Oceanography Laboratory. Nutrient concentrations were measured with an Auto-analyzer 3 (Seal Analytical, Segensworth, Hampshire, UK) following the methods delineated by Tréguer & Le Corre (1975).

POC and PON were determined on homogenized sediment trap material, selected ice and water samples, after filtration on pre-combusted Whatman GF/F filters.

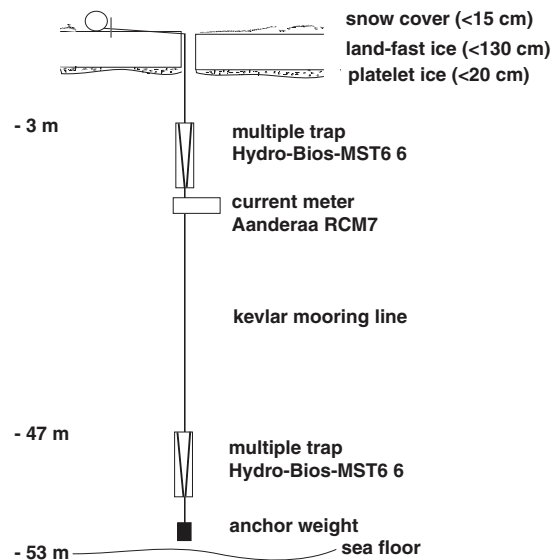


Fig. 4 Sediment traps and current meter mooring line deployed at station R1 from 8 November 2001 to 6 December 2001 in Pierre Lejay Bay.

The filters were then acidified with 37 % HCl vapours for 8 h, dried at 50°C and stored in a dessicator with drierite for later analyses on a Perkin Elmer 2400 Series II CHNS/O Elemental Analyzer following the modified Delmas method described by Jacobs (2006).

Cell counts and identification. All Bi, Pi and UIW5 samples were preserved in acidic Lugol's solution for the identification and enumeration of microalgae (Parsons et al. 1984). Cells were identified to the lowest possible taxonomic rank or were grouped together at the class or genus level, and enumerated under a Wild Heerbrugg inverted microscope (Leica Geosystems, Heerbrugg, Switzerland) operating with phase-contrast optics (Lund et al. 1958). Empty diatom cells were counted separately as centric or pennate forms. The following sources aided in the identification of the ice algae: Manguin (1957, 1960), Priddle & Fryxell (1985), Medlin & Priddle (1990), Hasle et al. (1994), Hasle & Syvertsen (1996) and Scott & Marchand (2005).

Diversity indices and multivariate analyses. The diversity of microalgal species was computed using the Simpson's (D) and Shannon (H') indices, with some methodological biases: (1) rare taxa were underestimated (no survey of rare taxa at low magnification) and (2) several taxa were not recognized at the species level but grouped together under a larger category such as the flagellates (the high diversity of archaeomonads, grouped in this article under the generic name *Archaeomonas* [cysts], has been detailed in the study by Riaux-Gobin & Stumm [2006]). Furthermore, several taxa (i.e., the nanoflagellates) were grouped into length categories. Microalgae not identified at species level (mostly flagellated cells) were grouped in morphometric size classes and were included in the multivariate analyses.

A multidimensional scaling (MDS) ordination based on Euclidean distances on standardized and $\log(x+1)$ -transformed environmental variables (nutrients, pigments, salinity, pH) was applied to the 32 Bi, Pi and UIW5 samples (Clarke & Warwick 2001). Similarities were computed among all pairs of samples on the basis of their taxonomic composition using the Bray–Curtis similarity coefficient (Bray & Curtis 1957). The break-down of species similarities, using the similarity of percentage (SIMPER) method, was calculated to determine which species contribute most for the similarity/dissimilarity within or between groups Bi, Pi and UIW5. A hierarchical cluster analysis was performed based on similarity between species to identify species

that present a similar ice-algal pattern distribution. Only contributions exceeding 5% were taken into account. The relationships between the species and the environmental variables were tested using the BIO-ENV procedure (Clarke & Warwick 2001). All analyses were performed using PRIMER software (Clarke & Warwick 2001).

Results

Sea-ice and atmospheric conditions

The consolidated land-fast ice at station R1 off Pierre Lejay Bay had a maximum thickness of 1.40 m measured in early November, with a thin Pi layer that was on average 0.20 m thick. The Bi horizon consists of granular ice colonized by sympagic algae over a thickness of 1–5 cm. The Pi thickness varied from 0.20 m at the coast to 0.30–0.40 m at 6-km offshore (data not shown). The land-fast ice was in place until the end of November 2001 and extended on average 80 km in front of the Dumont d'Urville Station (Fig. 2a). A large ice-free area was observed between the pack and land-fast ice until 22 November, when strong katabatic winds from the continent enlarged this polynya. The ice break-up started 30–40 km offshore on 4 December (Fig. 2b, c). On 1 January 2002 (Fig. 2d), the ice break-up was visible along a large part of the coast. The final dislocation of the 1 m thick land-fast ice in Pierre Lejay Bay occurred on 10 January under a noticeable swell (pers. obs.; no swell recorder) and strong wind from the east.

The fast-ice thickness at R1 (Fig. 5) slowly decreased from 1.32 m on 3–5 November to 1.00 m on 29 December. The snow cover decreased from 0.10 to 0.00 m (Fig. 5), albeit with several brief increases due to new precipitation (i.e., around days 36 and 50). The ice surface became soft and porous by 27 December but without melt ponds. The Bi horizon also softened and became unstable at that time while the Pi remained present at R1 with around the same thickness ($0.20 \text{ m} \pm 0.1$) during the entire study period. The Pi was deeply coloured by sympagic algae by 23 November. After 29 December, the ice began to rot throughout, making travel on the fast ice unsafe, so sampling was discontinued.

The mean air temperature progressively increased from -14°C in early November 2001 to above freezing point in late December (Fig. 3). Six consecutive days with positive temperatures characterized the time between the end of December and the beginning of January. A new record in maximum air temperature (9.9°C) was measured on 30 December 2001.

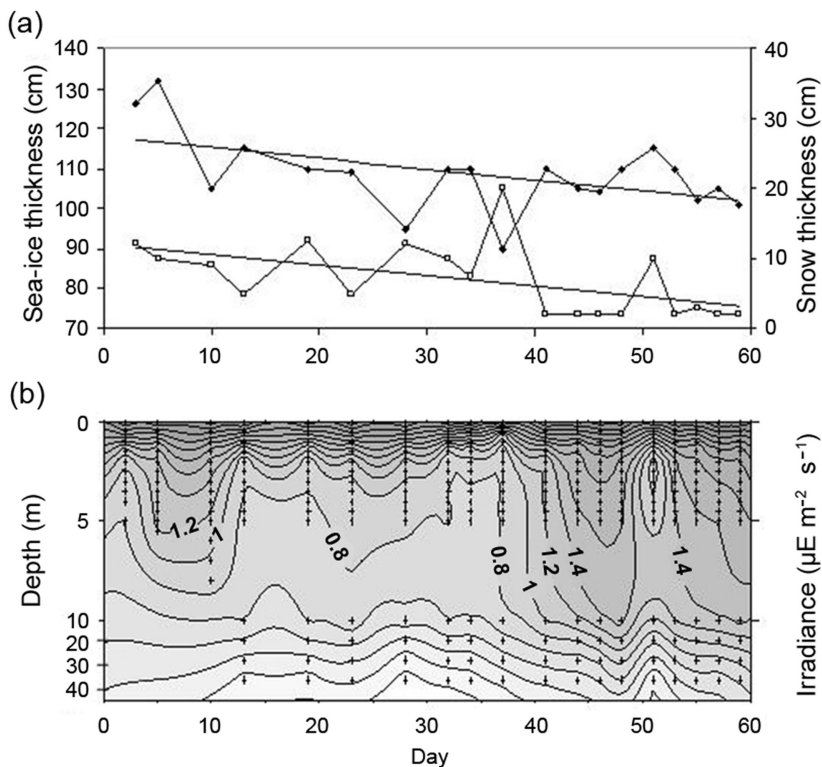


Fig. 5 Temporal variation of (a) ice thickness ($y = -0.2704x + 118R^2 = 0.2655$) and snow ($y = -0.1492x + 12.011R^2 = 0.2762$), and (b) sub-ice irradiance ($\mu E m^{-2} s^{-1}$) at station R1 in Pierre Lejay Bay from 1 November 2001 (day 1) to 29 December 2001 (day 59). Diamond: ice thickness; square: snow depth.

Sub-ice oceanic short-term regime

Sub-ice daily salinity–temperature profiles (0–50 m) at R1 are shown in Fig. 6. The range of variations over 48 days is more important than the one observed during a single tidal cycle (two tidal cycles with different tidal amplitudes were sampled on 8–9 December and 11–12

December; data not shown). A time trend of the data obtained during the conductivity–temperature–density profiles taken at regular intervals ($y = 0.663x + 35.669$, $R^2 = 0.2913$, temperature [x] in °C, salinity [y] in psu; trend not shown in Fig. 6) suggests a progressive warming of the water masses over the sampling period together with an increase in salinity. At the start of the time series,

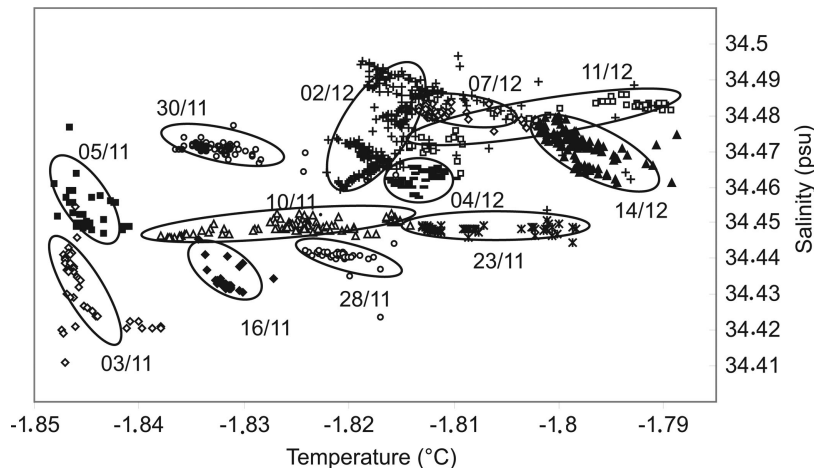


Fig. 6 Relationship between temperature and salinity profiles recorded at station R1 in Pierre Lejay Bay from 3 November to 14 December 2001. Each ellipse represents a daily salinity–temperature profile.

colder and less saline waters were recorded, while in the last four profiles, a stratification with more saline and warmer water developed below 20–30 m (data not shown).

The snow cover at R1 decreased more or less progressively from more than 0.10 m at the beginning of November to near zero after 10 December, in parallel with the ice ablation (Fig. 5). The mid-day irradiance sharply increased after 10 December (day 40) and reached up to 1–1.4 $\mu\text{E m}^{-2} \text{s}^{-1}$ at 10–30 m water depth. Directly under the Bi (0 m), the irradiance was $>3 \mu\text{E m}^{-2} \text{s}^{-1}$ after day 45 (Fig. 5b). There was a temporary decrease related to a snowfall event during a short period around 21 December (day 52; Fig. 5b).

Physical oceanography. The tides in Pierre Lejay Bay are composed of two irregular daily oscillations (Fig. 3). During the study period, the maximum tidal amplitude was 2.2 m and the maximum current speed was 35 cm s^{-1} . Maximum current speed events were associated with the mid-flood and mid-ebb periods of the maximal daily oscillation (data not shown). The coastal surface currents were directly under the influence of the tidal regime. The reverse between ebb and flood was sudden, with a short but strong northern component just before the flood and a high reproducibility between consecutive tidal cycles (data not shown).

The progressive vector of currents (Fig. 7) showed two major components: east–north–east (from A to B and from C to D) and west–north–west (from B to C and from D to E); these two major directions of the drift were related to neap tides (east–north–east drift) and spring tides (west–north–west drift). Further registrations would help in understanding the exact parameters forcing the changes in drift directions: B, C and D in Fig. 7 are roughly located at the start and the end of the spring tide period.

Land-fast ice geochemistry before the spring break-up

Ice and sub-ice 2001 time series. Average and range values of physical, chemical and biological variables from Bi, Pi and UIW5 at R1 during the study period are summarized in Table 1. Temporal variations in salinity, $\text{Si}(\text{OH})_4$, NO_2^- , $\text{NO}_3^- + \text{NO}_2^-$, PO_4^- , Chl *a*, Phaeo *a* and pH before the ice break-up are illustrated in Figs. 8 and 9.

A steady decrease in salinity was obvious in all layers (Bi, Pi) and UIW5 during the days preceding the ice break-up (days 47–59; Fig. 8a), even if less marked for the Bi. After day 30, the Chl *a* biomass in the Bi increased (Fig. 9b), but with no regular trend, and reached

2.6 mg l^{-1} (i.e., 130 mg m^{-2}). The Chl *a* concentration was on average 0.6 mg l^{-1} during the 70 days preceding the ice break-up (i.e., 30 mg m^{-2} , Table 1). The POC concentration averaged 20 mg l^{-1} (i.e., 1 g m^{-2} ; data not shown) in the Bi horizon. These values were positively related from day 35 to an increase in under-ice irradiance until the ice break-up (Fig. 5b). Note the great temporal variations in the ice algal biomass (Fig. 9) and in the succession of the different microalgal taxa (Figs. 11–13).

PO_4^- concentrations, reaching a maximum of $51 \mu\text{M}$ in Bi and $38 \mu\text{M}$ in Pi at day 55, showed a co-variation with Chl *a* (Fig. 9a, b). High silicic acid concentrations of $>70 \mu\text{M}$ at 5-m water depth at the end of the time series, and at 10 and 20 m in the underlying water masses (data not shown) characterized the sub-ice water while low values were recorded in the ice (particularly the Bi, i.e., $5\text{--}7 \mu\text{M}$), suggesting a possible biological depletion (Fig. 8b). The $\text{Si}(\text{OH})_4$ concentrations at 5 m clearly increased from day 30 (Fig. 8b), whereas $\text{NO}_3^- + \text{NO}_2^-$ concentrations were high throughout the study, particularly at the end of the time series, where it reached $67 \mu\text{M}$ in the Pi horizon. Nitrite (Fig. 8c) was related to pigment degradation in Bi and Pi horizons before the ice break-up when Phaeo *a* reached $850 \mu\text{g l}^{-1}$ at the end of the time series (Fig. 9c). The pH values ranged from 7.2 to 8.4, without any specific trend, except for slightly lower values in the Bi horizon towards the end of the time series (Fig. 9d). Graphically represented in an MDS ordination, the environmental variables

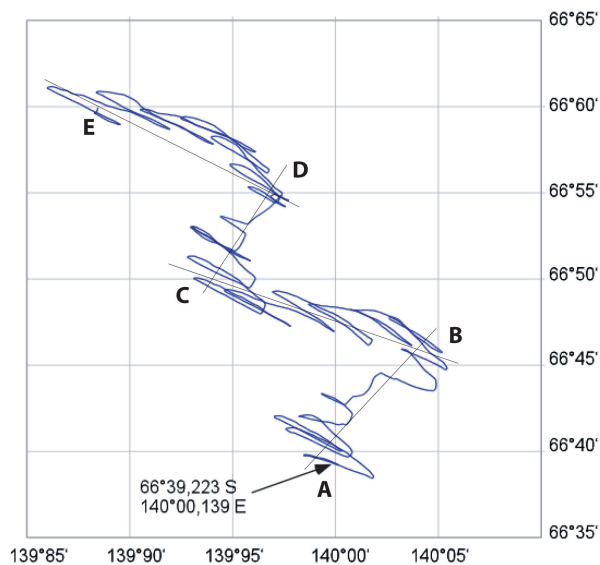


Fig. 7 Progressive vector of currents recorded at 3 m depth under the land-fast ice at station R1 in Pierre Lejay Bay from 1 November (day 1) to 29 December 2001 (day 59). Letters A–E correspond to directional changes of the drift in relation with the tidal amplitude.

Table 1 Environmental and biological variables (mean \pm standard deviation) recorded at station R1 in Pierre Lejay Bay from 1 November (day 1) to 29 December 2001 (day 59) in the bottom ice (Bi, 19 samples), platelet ice (Pi, 19 samples) and sub-ice water at 5 m depth (UIW5, 15 samples).

Variable	Bi		Pi		UIW5	
	min-max	Mean \pm SD	min-max	Mean \pm SD	min-max	Mean \pm SD
pH	6.8–8.7	7.5 \pm 0.6	7.6–8.2	7.9 \pm 0.3	7.7–8.2	7.9 \pm 0.2
Salinity	2.6–7.9	4.9 \pm 1.6	17.2–27.9	22.4 \pm 3.5	33.3–34.1	34.0 \pm 0.2
Chl ^a a (μ g l ⁻¹)	65–2557	646 \pm 659	17.1–715	253 \pm 206	0.3–1.9	0.7 \pm 0.5
Chl ^a c (μ g l ⁻¹)	14.7–512	136 \pm 144	3–170	56 \pm 48	0.04–0.34	0.1 \pm 0.1
Phaeo ^b a (μ g l ⁻¹)	0–849	89 \pm 237	0–218	29 \pm 52	0.03–0.16	0.1 \pm 0.0
NO ₂ ^{-c} (μ M)	0.04–0.24	0.1 \pm 0.1	0.04–0.35	0.2 \pm 0.5	0.01–0.18	0.1 \pm 0.1
NO ₃ ⁻ +NO ₂ ^{-d} (μ M)	6.0–39	21.1 \pm 11.8	9.9–67	26.9 \pm 13.9	9.8–33	21.3 \pm 9.0
PO ₄ ^{-e} (μ M)	0.5–51	14.2 \pm 14.5	1.4–37.9	9.4 \pm 9.8	0.9–2.0	1.4 \pm 0.5
Si(OH) ₄ ^f (μ M)	3.7–18.3	7.5 \pm 3.6	19.6–53	31.2 \pm 10.2	28–74	49.1 \pm 17.9
POC ^g (mg l ⁻¹) ^h	–	15.4 \pm 8.8	–	20.6 \pm 7.9	–	0.3 \pm 0.1
PON ⁱ (mg l ⁻¹) ^h	–	2.2 \pm 1.5	–	3.1 \pm 1.3	–	0.1 \pm 0.0
C:N ^{j,h}	–	8.4 \pm 1.2	–	8.3 \pm 2.9	–	14.2 \pm 2.8

^aChlorophyll.^bPhaeopigment.^cNitrite.^dNitrate + nitrite.^ePhosphate.^fSilicic acid.^gParticulate organic carbon.^hSample numbers: Bi 4; Pi 14; UIW5 3.ⁱParticulate organic nitrogen.^jAtomic ratio.

(nutrients, pigments, salinity, pH) clearly discriminated three groups of samples consisting of Bi, Pi and UIW5 (Fig. 10). This analysis confirmed the probable distinctive origin of Bi and Pi, and supports the observed differences in time variation in the three horizons.

POC and PON concentrations in the Bi and Pi horizons varied from 15 to 21 mg l⁻¹ and from 2 to 3 mg l⁻¹, respectively. They are 10–20 times higher than in the sub-ice waters (Table 1). The C:N ratio, averaging around 8 in the ice horizons was lower than in UIW5 (14.2).

Sub-ice particle flux. The POM flux at R1 remained stable during the sediment trap experiment although there was a sharp increase in the last cup, 33 days before the effective ice break-up (Table 2). In the near-surface trap at 3 m under the ice (Fig. 4), the pigment concentrations increased slowly and more or less regularly from 8 November (day 10), but more strongly after 2 December (day 34), with a concentration 10 times higher than at the beginning of the trap experiment. In the bottom trap, at 6 m above the seafloor, all pigment concentrations were higher than those measured directly under the ice and here again after 2 December the pigment concentration was six times higher than at day 10. The Chl a :Phaeo a ratio was surprisingly high (> 0.9) and higher in the bottom (1.5–2.0) than in the surface trap (0.9–1.3). It did not significantly vary with time. The

Chl c :Chl a ratio varied similarly with time on the two traps (Table 2) and its mean value (on average 0.19) was not so different than in the Bi (on average 0.21) and Pi (on average 0.22) sympagic communities (Table 1, ratio not detailed). POC and PON also increased in the two sediment traps with maximum values of 62 and 16 mg m⁻² d⁻¹, respectively, in the surface layer and slightly higher rates at 47-m depth (79 and 24 mg m⁻² d⁻¹). The C:N ratio was very low (2.4–5.0, Table 2) in comparison to the values recorded in sea ice or UIW5 (8.3–14.2, Table 1) and with the more classical Redfield ratio in phytoplankton (6.6; see Redfield et al. 1963).

The trap material contained few zooplankton, attesting to a possible low sub-ice level of grazing near the continent shelf, as previously recorded by Honjo (2004) in the Ross Sea Gyre. A mini-remotely operated vehicle (ROV) survey under the land-fast ice near R1 in 2007 found no krill (G.S. Dieckmann, pers. obs.), supporting the suggestion of a low grazing pressure in this area, irrespective of the sampling year.

From the maximum particle flux at R1 (Table 2), it is difficult to extrapolate to an annual flux value since the duration of the most intense events, that started several weeks before the ice break-up at coast, is unknown. Nevertheless, we can consider that in 2001/02, the total rate in Pierre Lejay Bay must have been ≥ 7 g POC m⁻² yr⁻¹, with a potential active sedimentation

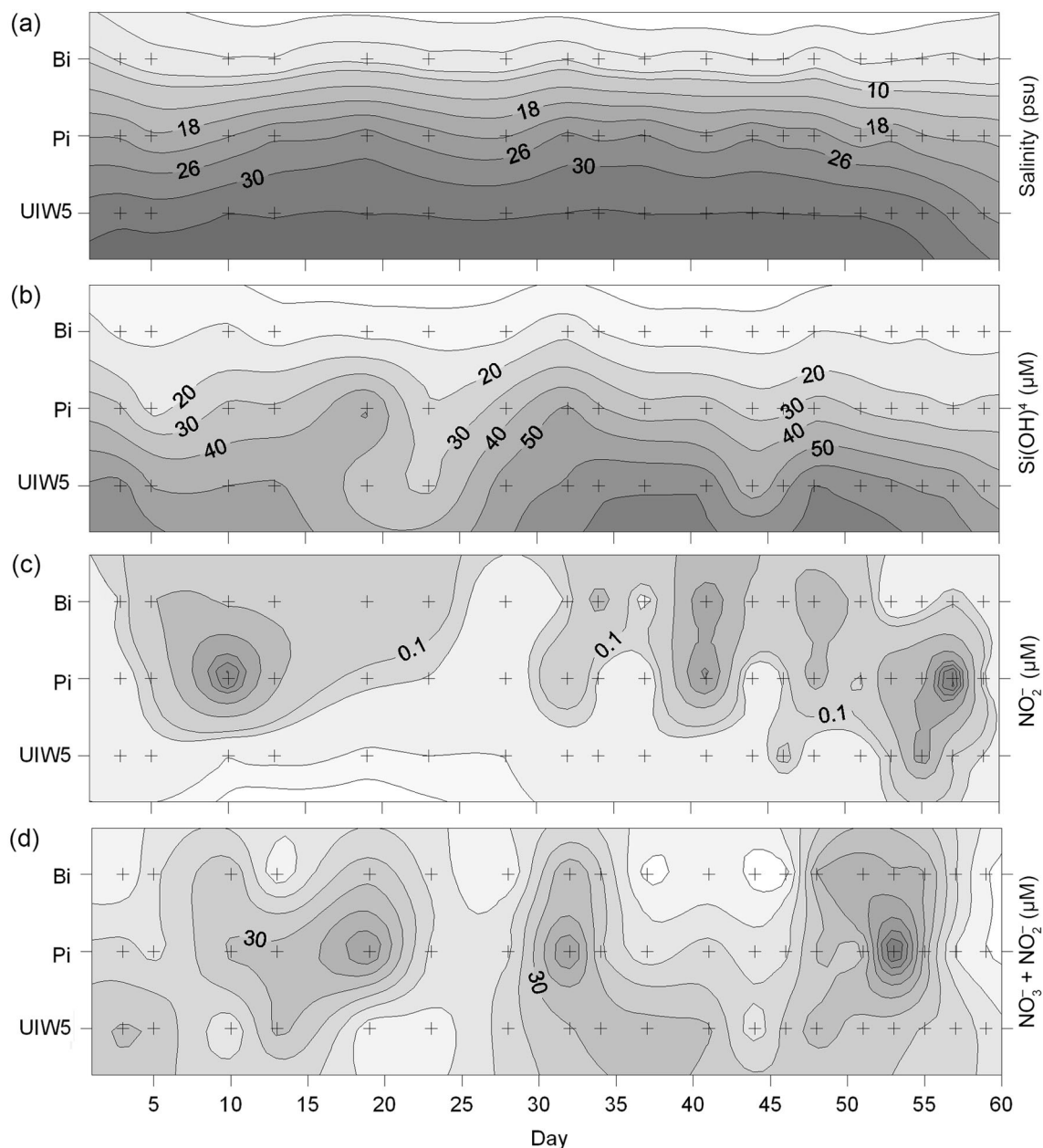


Fig. 8 Temporal variations of (a) salinity, (b) silicic acid (Si(OH)_4), (c) nitrite (NO_2^-) and (d) nitrate plus nitrite ($\text{NO}_3^- + \text{NO}_2^-$) in bottom ice (Bi), platelet ice (Pi) and sub-ice water at 5 m depth (UIW5) at station R1 in Pierre Lejay Bay from 1 November (day 1) to 29 December 2001 (day 59).

period of three months around the ice break-up (see Discussion section).

Taxonomic composition and time succession.

Microalgae recorded in the Bi, Pi and UIW5 are presented in Table 3 while the successions of major protist groups and species can be viewed in Figs. 11–13. The similarities and dissimilarities (SIMPER) between Bi, Pi and at UIW5 are presented in Tables 4 and 5.

Four diatom taxa, namely *Berkeleya adeliensis*, *Cylindrotheca closterium*, *Nitzschia leointei* and *N. stellata*, were preferentially associated with the Bi horizon reaching abundances of 21×10^8 cells m^{-2} , 90×10^6 cells m^{-2} , 19.5×10^7 cells m^{-2} and 17.5×10^8 cells m^{-2} , respectively, while *Navicula glaciei*, with 49×10^8 cells m^{-2} , and *Amphiprora kufferathii*, with 15×10^6 cells m^{-2} , were better adapted to the Pi horizon (Figs. 11, 12). *Berkeleya adeliensis* and *Fragilariopsis cylindrus* first occurred in the Bi with 16×10^7 cells m^{-2} for *F. cylindrus*, but later

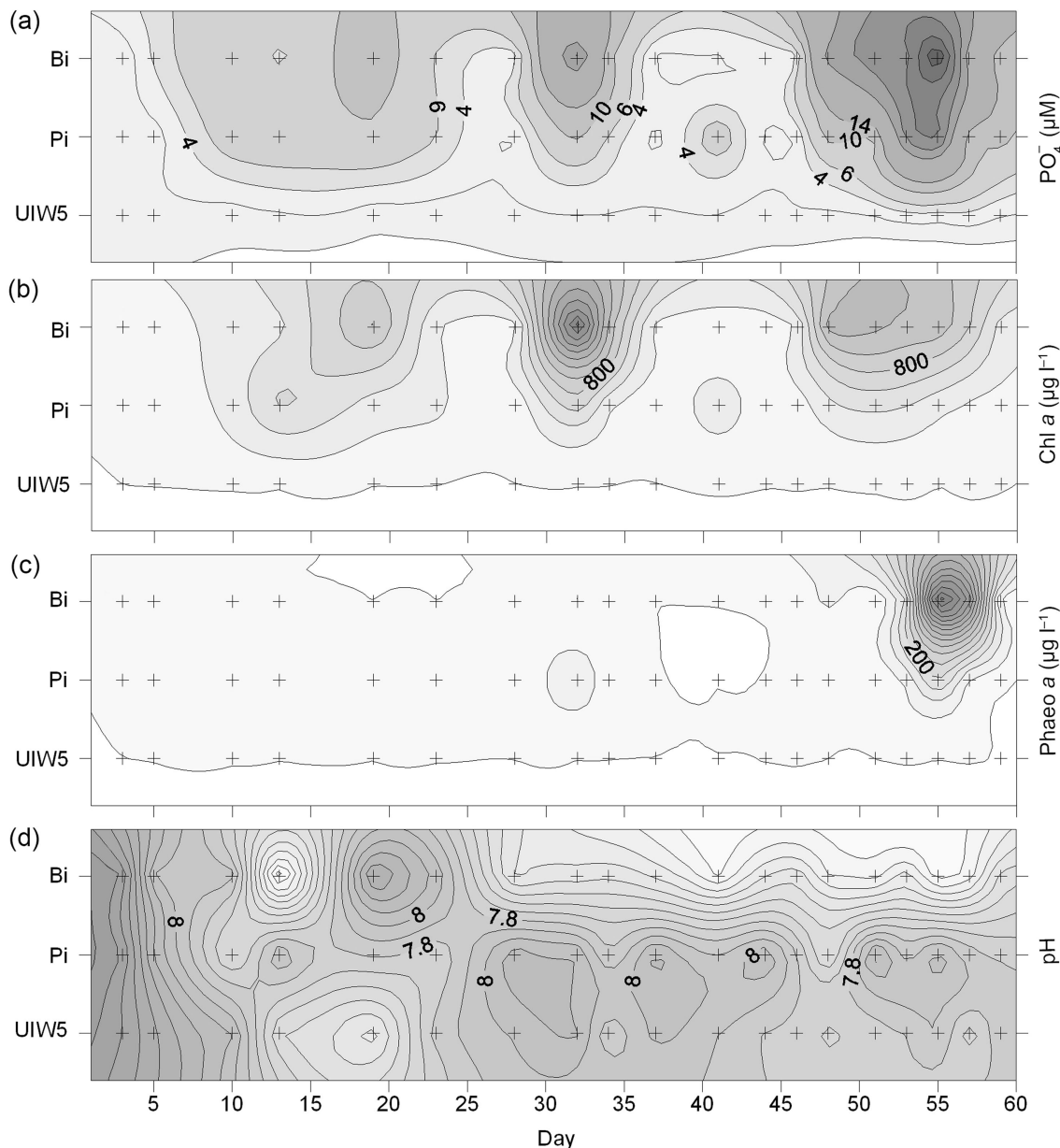


Fig. 9 Temporal variations of (a) phosphate (PO_4^-), (b) chlorophyll (Chl) α , (c) phaeopigment (Phaeo) α concentrations and (d) pH in bottom ice (Bi), platelet ice (Pi) and sub-ice water at 5-m depth (UIW5) at station R1 in Pierre Lejay Bay from 1 November (day 1) to 29 December 2001 (day 59).

colonized the Pi horizon (Fig. 12). The same differentiation in colonization between Bi and Pi can be observed for the nanoflagellates (Fig. 13).

Interestingly, centric diatoms occurred more frequently in the Pi than Bi horizon (Table 3), while the pennate genera *Haslea* Simonsen and *Plagiotropis* Pfitzer were more common in the Bi horizon and flagellates from the UIW5 depth. Furthermore, several algal taxa were only present in the UIW5, such as some Dinophyceae, *Entomoneis oestrupii*, *Fragilariopsis obliquocostata* and *Pyramimonas nansenii* (Table 3). Gymnodinioid taxa were

encountered in sub-ice waters, probably developing a heterotrophic strategy or specific adaptation to low light, while the archaeomonads were present in all sea-ice horizons but far less abundant at 5 m depth.

The reported diatom diversity was relatively low, in part due to the methodology. The Shannon (H') index averaged 1.63 in the Bi, 1.60 in Pi and 1.89 at UIW5. The H' index slightly increased over time in the Pi horizon and UIW5 (data not shown).

A succession in the sympagic communities was obvious for diatoms and other microalgal taxa (Figs. 11–13).

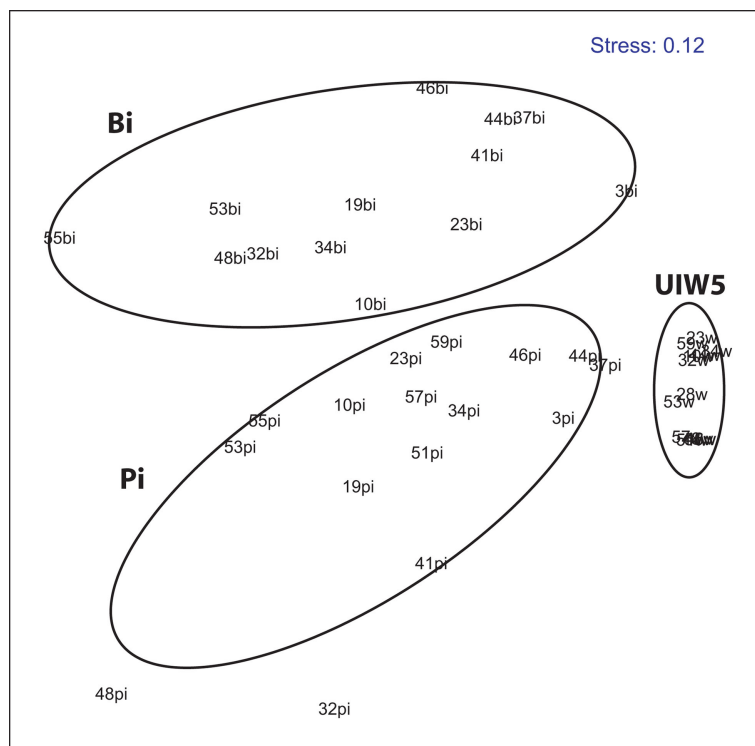


Fig. 10 Two-dimensional non-metric multidimensional scaling (MDS) of 40 samples based on standardized and log ($x+1$)-transformed selected variables (nutrients, pigments, salinity, pH), with three groups delineated: bottom ice (Bi), platelet ice (Pi) and 5 m sub-ice water (UIW5).

Among the dominant species, *Amphiprora kufferathii*, *Cylindrotheca closterium*, *Navicula glaciei* and *Nitzschia lecointei* reached maximum cell abundance during the first half of November (Fig. 11), while *Fragilariopsis cylindrus*, *F. sublinearis*, with 28×10^6 cells m^{-2} , and *Nitzschia stellata*, with 92×10^8 cells m^{-2} , reached their higher abundance in the second half of that month (Fig. 12). Other taxa, such as *Berkeleya adeliensis* and *Fragilariopsis curta*, with 35×10^5 cells m^{-2} , were dominant for a few weeks before the ice break-up. Nano-flagellates were more abundant towards the end of November in the Bi horizon, reaching 26×10^8 cells m^{-2} , while gymnodinioid dinoflagellates ($< 20 \mu m$) were increasing in number in the Bi by mid-December (Fig. 13). The prymnesiophyte *Phaeocystis antarctica*, reaching 3.6×10^6 cells m^{-2} , grew preferentially in the Pi and at UIW5, but only during the last 10 days before the ice break-up (Fig. 13d).

The clustering analysis (Fig. 14) discriminated two groups, one composed of *Phaeocystis antarctica*, *Fragilariopsis curta* and gymnodinioid cells ($< 20 \mu m$), which were characteristic of the UIW5 depth, and one composed of 10 other diatom taxa and nanoflagellates ($< 10 \mu m$).

The centric and pennate empty frustules were not included in the analyses but 54% of the total diatom

population at UIW5 consisted of empty cells, with maximum values from day 20 to day 50. This percentage was lower but extremely variable (from 1% to exceptionally 40%) in the Bi and Pi horizons and increased slightly until the ice break-up, but with no direct relationships with the degraded pigment concentrations (Phaeo a).

Some correlation analyses between microalgal species and different subsets of environmental variables (BIOENV analysis) showed that Chl a and c concentrations were highly correlated to the Phaeo b concentrations, and between themselves ($R > 0.90$, $p < 0.001$ in all cases), and were therefore excluded from the analysis (Clarke & Warwick 2001). The structure of the microalgal communities was explained by the best three-variable combination ($R = 0.68$), corresponding to salinity, Phaeo b and PO_4^- concentration.

Discussion

Spatial heterogeneity

In the vicinity of the Dumont d'Urville Station, the land-fast ice thickness was relatively consistent between years (Riaux-Gobin et al. 2000; Riaux-Gobin et al. 2005).

Table 2 Variables measured from the material collected on the sediment traps deployed from 8 November to 6 December 2001 at station R1 in Pierre Lejay Bay.

Deployment time	Duration (h)	Depth (m)	Chl ^a α ($\mu\text{g m}^{-2} \text{d}^{-1}$)	Chl ^a c ($\mu\text{g m}^{-2} \text{d}^{-1}$)	Phaeo ^b α ($\mu\text{g m}^{-2} \text{d}^{-1}$)	Chl ^a c :Chl ^a α ratio	Chl ^a α :Phaeo ^b α ratio	POC ^c ($\text{mg m}^{-2} \text{d}^{-1}$)	PON ^d ($\text{mg m}^{-2} \text{d}^{-1}$)	POC ^c :Chl ^a w/w ratio	C:N ^e
8 Nov–14 Nov	144	3	32.1	5.3	34.1	0.16	0.9	14.1	6.9	438	2.4
14 Nov–20 Nov	144	3	60.1	16.2	55.2	0.27	1.1	20.8	–	347	–
20 Nov–26 Nov	144	3	65.5	17.6	50.3	0.27	1.3	24.6	–	376	–
26 Nov–2 Dec	144	3	55.4	8.8	44.4	0.16	1.3	10.6	3.7	191	3.3
2 Dec–6 Dec	88	3	569.7	74.2	466.4	0.13	1.2	62.1	16.0	109	4.5
8 Nov–14 Nov	144	47	82.0	16.1	41.6	0.20	2.0	15.9	3.7	194	5.0
14 Nov–20 Nov	144	47	85.4	21.5	45.6	0.25	1.9	15.2	4.2	178	4.2
20 Nov–26 Nov	144	47	114.3	25.6	74.7	0.22	1.5	25.2	–	220	–
26 Nov–2 Dec	144	47	107.7	18.1	56.3	0.17	1.9	21.2	5.6	197	4.4
2 Dec–6 Dec	88	47	646.6	75.2	391.7	0.12	1.7	78.6	24.1	122	3.8

^aChlorophyll.^bPhaeopigment.^cParticulate organic carbon.^dParticulate organic nitrogen.^eAtomic ratio.

The spatial heterogeneity was tested at R1 in 1999 while the fast-ice conditions were similar to that experienced in 2001 (Riaux-Gobin et al. 2000; Riaux-Gobin et al. 2005). The test took place on a large surface (average 625 m²), following a “Latin Square” pattern (Table 6). Each of the five coring points was sampled twice (duplicates at 3-m intervals). Data were not homogeneous across the sampled area, which was probably related to the differences in snow cover or irregularity in ice thickness, while the duplicates showed a lower variability (Table 6). To reduce the impact of the patchiness, the 2001 time series took place on a reduced area (see Sampling site, material and methods section).

Conditions before the break-up, interannual variation

During the austral spring of 2001, the biochemical conditions of the land-fast ice prior to the break-up were relatively similar to those reported from the same Dumont d’Urville sampling site in 1995 and 1999 (Riaux-Gobin et al. 2005). The temporal variation of the nutrient and pigment concentrations matched those previously recorded (Riaux-Gobin et al. 2000; Riaux-Gobin et al. 2005). However, there were some differences that can be linked to the year’s conditions. For instance, the absence of early winter break-up events in 2001 may have caused the exceptionally high thickness of the ice and delayed the timing of the break-up in early 2002 when compared with the timing in 1995 and 1999 (Riaux-Gobin et al. 2005).

The 2001 nutrient concentrations were lower than those recorded at the same station R1 in 1995 (300 $\mu\text{M NO}_3^-$ in Pi) but similar to 1999 (Riaux-Gobin et al. 2005). Fiala et al. (2006) reported much lower nutrient and algal biomass concentrations in 1998 at station C, near to R1, with 10–12 $\mu\text{M NO}_3^-$ and 50–90 $\mu\text{g Chl } a \text{ l}^{-1}$ in the Bi horizon, highlighting the interannual variability in the measured parameters. The decoupling between the silicon cycle and the nitrogen cycle (Riaux-Gobin et al. 2000; Riaux-Gobin et al. 2005) was confirmed by the present data set. A decoupling between the silicon and the phosphorus cycles (Figs. 5, 7) is also highlighted. High PO_4^- concentration in the Bi horizon reaching 51 μM at the end of this study is indicative of a mineralization of the organic matter (Arrigo et al. 1995; Günther et al. 1999). Nitrification concurrently took place in Bi and Pi while the under-ice water was enriched with NO_2^- at the end of the study. Si(OH)_4 was depleted in the 2001 ice horizons and showed high concentrations at 5 m depth, corroborating previous reports (Riaux-Gobin et al. 2000; Riaux-Gobin et al. 2005).

Table 3 Protist taxa reported from the bottom ice (Bi), platelet ice (Pi) and in the sub-ice water at 5 m depth (UIW5) at station R1 in Pierre Lejay Bay from 1 November (day 1) to 29 December 2001 (day 59). The species name abbreviations are those used in Fig. 11.

		Bi	Pi	UIW5
BACILLARIOPHYTA				
Centrales				
accu	<i>Actinocyclus curvatulus</i> Janisch	–	x	–
chsp	<i>Chaetoceros</i> sp.	–	x	–
cocr	<i>Corethron criophilum</i> Castracane	x	x	–
daan	<i>Dactyliosolen antarcticus</i> Castracane	–	x	–
odli	<i>Odontella litigiosa</i> (Van Heurck) Hoban	–	x	–
odwe	<i>O. weissflogii</i> (Janisch) Grunow	–	–	x
pops	<i>Porosira pseudodenticulata</i> (Hustedt) Jousé	–	x	–
thsp	<i>Thalassiosira</i> sp.	–	x	–
Pennates				
amku	<i>Amphiprora kufferathii</i> Manguin	x	x	x
amsp	<i>A.</i> sp.	–	x	–
amba	<i>Amphora barreii</i> Manguin	–	x	–
babe	<i>Banquisia belgicae</i> (Van Heurck) Paddock	x	x	x
bead	<i>Berkeleya adeliensis</i> Medlin	x	x	x
cycl	<i>Cylindrotheca closterium</i> (Ehrenberg) Reimann and Lewin	x	x	x
enkj	<i>Entomoneis kjellmanii</i> (Cleve) Poulin and Cardinal	x	x	x
enoe	<i>E. oestrupii</i> (Van Heurck) Cremer	–	–	x
enpa	<i>E. paludosa</i> var. <i>hyperborea</i> (Grunow) Poulin and Cardinal	–	x	–
frcu	<i>Fragilariopsis curta</i> (Van Heurck) Hustedt	x	x	x
frcy	<i>F. cylindrus</i> (Grunow ex Cleve) Frenguelli	x	x	x
frob	<i>F. obliquecostata</i> (Van Heurck) Heiden	–	–	x
frsu	<i>F. sublinearis</i> (Van Heurck) Heiden	x	x	x
hama	<i>Haslea major</i> (Heiden) Simonsen	x	–	–
hatr	<i>H. trompii</i> (Cleve) Simonsen	x	–	–
mari	<i>Manguinea rigida</i> (M. Peragallo) Paddock	–	x	–
nadi	<i>Navicula directa</i> (W. Smith) Ralfs	x	x	x
nagl	<i>N. glaciei</i> Van Heurck	x	x	x
nasp	<i>N.</i> sp.	x	x	x
nasp	<i>N.</i> sp. 1	x	x	x
nile	<i>Nitzschia lecointei</i> Van Heurck	x	x	x
nist	<i>N. stellata</i> Manguin	x	x	x
nisp	<i>N.</i> sp. 1	x	x	x
nita	<i>N. taeniiformis</i> Simonsen	x	x	x
plac	<i>Plagiotropis acuta</i> (M. Peragallo) Simonsen	x	–	–
plpa	<i>P. paddockii</i> Simonsen	x	–	–
pssu	<i>Pseudo-nitzschia subcurvata</i> (Hasle) Fryxell	x	–	–
pstu	<i>P. turgiduloides</i> (Hasle) Hasle	x	x	x
pssp	<i>P.</i> sp. 1	x	x	x
syre	<i>Synedropsis recta</i> Hasle, Medlin and Syvertsen	x	x	x
CHOANOFAGELLIDEA				
mosp	<i>Monosiga</i> sp.	–	x	x
CHRYSOPHYCEAE				
arcy	<i>Archaeomonas</i> (cysts)	x	x	x
diba	<i>Dinobryon</i> cf. <i>balticum</i> (Schütt) Lemmermann	x	x	–
CRYPTOPHYCEAE				
lesp	<i>Leucocryptos</i> sp.	x	x	x
rhsp	<i>Rhodomonas</i> sp.	–	–	x
DICTYOCOPHYCEAE				
disp	<i>Dictyocha speculum</i> Ehrenberg	–	x	x
DINOPHYCEAE				
amsp	<i>Amphidinium</i> cf. <i>sphenoides</i> Wulff	–	–	x
gyel	<i>Gymnodinium</i> cf. <i>elongatum</i> Hope	–	–	x
gyga	<i>G.</i> cf. <i>galeatum</i> Larsen	–	–	x

Table 3 Continued

		Bi	Pi	UIW5
gysp	<i>G. cf. spirale</i> (Bergh) Kofoid and Swezy	–	–	x
hesp	<i>Heterocapsa</i> sp.	–	–	x
oxgr	<i>Oxytoxum gracile</i> Schiller	–	–	x
prsp	<i>Protoperidinium</i> sp. 1	–	x	x
EUGLENOPHYCEAE				
eubr	<i>Eutreptiella braarudii</i> Thronsen	–	x	–
PRYMNESIOPHYCEAE				
phan	<i>Phaeocystis antarctica</i> Karsten	–	x	x
PRASINOPHYCEAE				
pyna	<i>Pyramimonas nansenii</i> Braarud	–	–	x

– = not detected.
x = present.

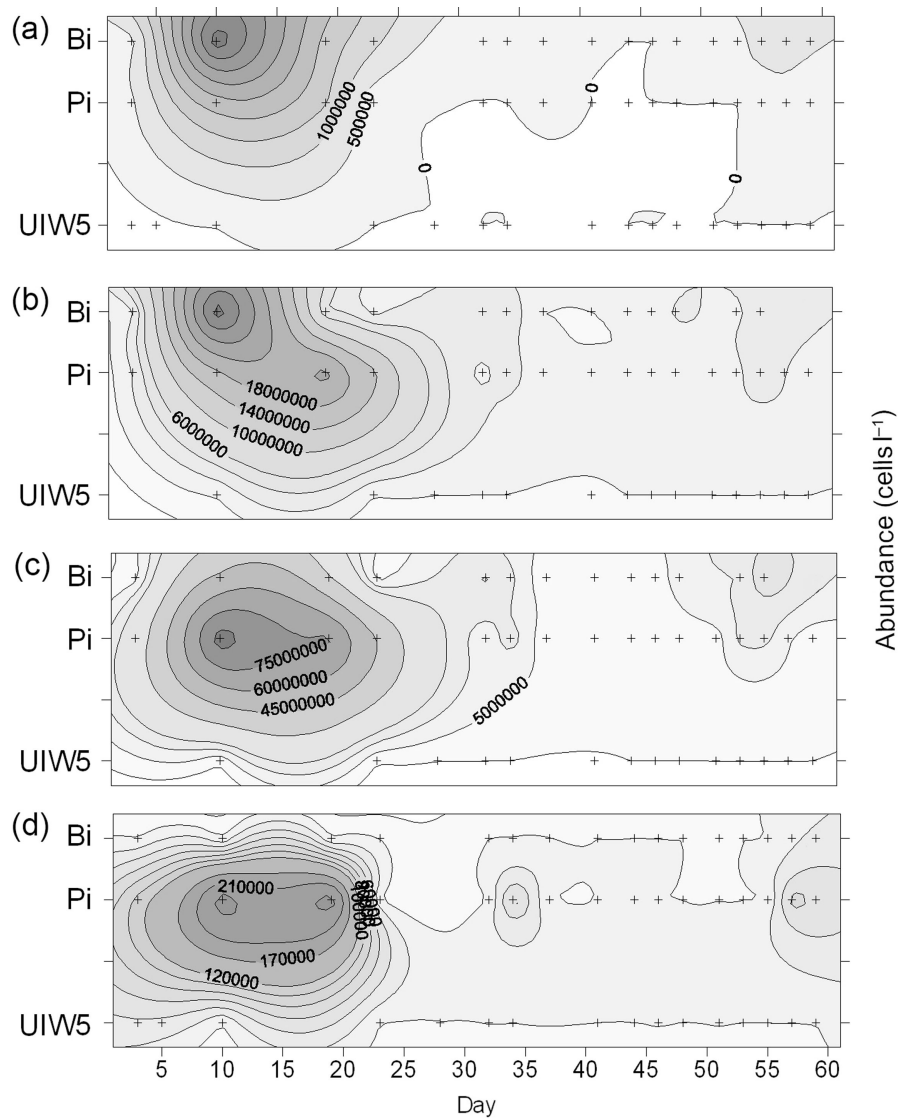


Fig. 11 Temporal variations in cell abundance of the dominant diatom species (a) *Cylindrotheca closterium*, (b) *Nitzschia lecontei*, (c) *Navicula glaciei* and (d) *Amphiprora kufferathii* in bottom ice (Bi), platelet ice (Pi) and sub-ice water at 5 m depth (UIW5) at station R1 in Pierre Lejay Bay from 1 November (day 1) to 29 December 2001 (day 59).

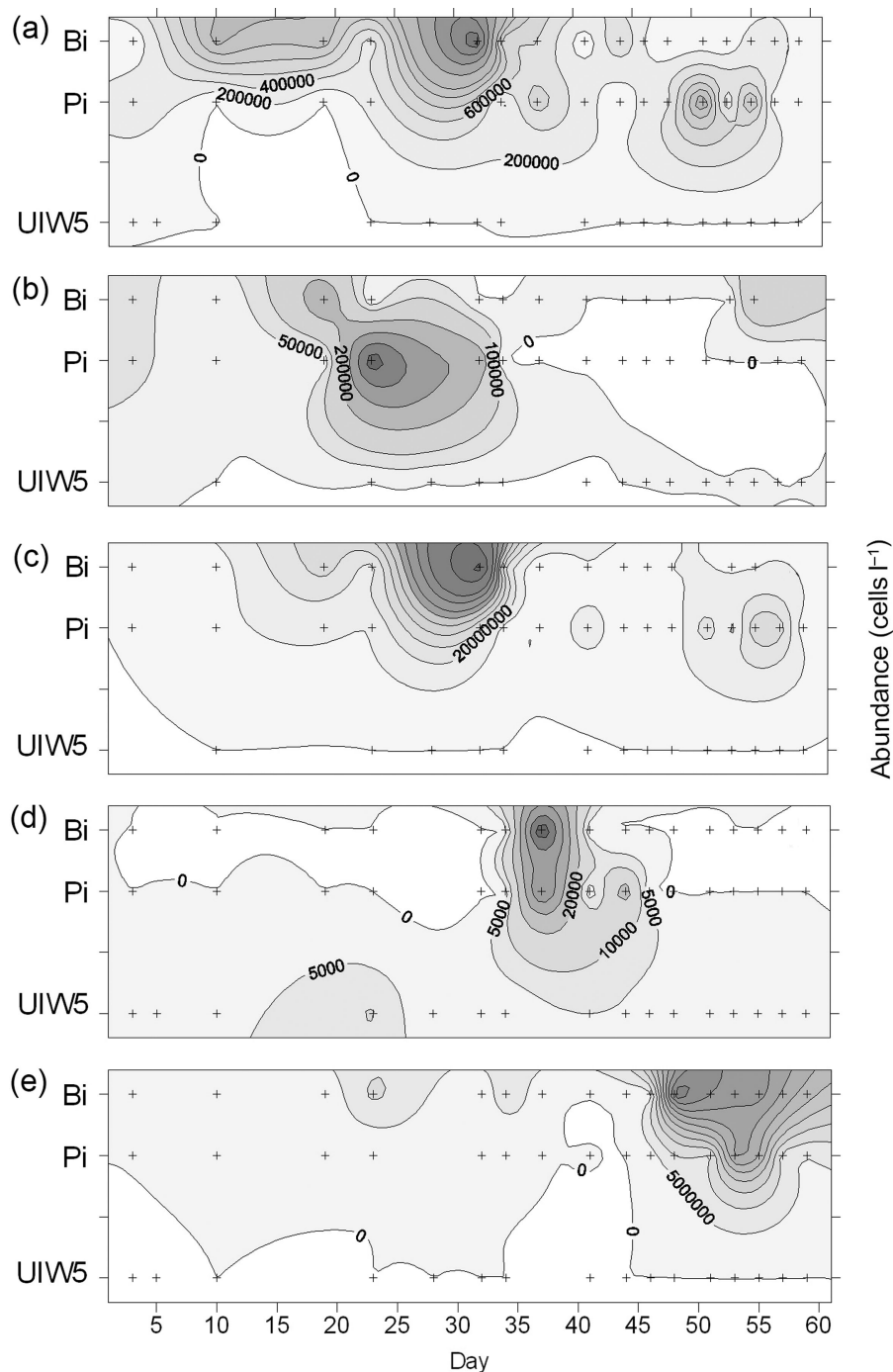


Fig. 12 Temporal variations in cell abundance of the dominant diatom species (a) *Fragilariopsis cylindrus*, (a) *F. sublinearis*, (c) *Nitzschia stellata*, (d) *Fragilariopsis curta* and (e) *Berkeleyya adeliensis* in bottom ice (Bi), platelet ice (Pi) and sub-ice water at 5 m depth (UIW5) at station R1 in Pierre Lejay Bay from 1 November (day 1) to 29 December 2001 (day 59).

Some interannual differences appeared in the microalgal colonization of the various ice horizons, which may be explained by their formation history. The maximum Bi Chl *a* biomass (130 mg m^{-2}) recorded in 2001 was close to that reported in 1999 ($87\text{--}187 \text{ mg m}^{-2}$;

Riaux-Gobin et al. 2005). Conversely, the maximum Chl *a* biomass in 1995— 1.9 g m^{-2} —was considerably higher but was recorded in the Pi horizon (Riaux-Gobin et al. 2005). This biomass difference between years can be partly explained by difference in ice thickness and its

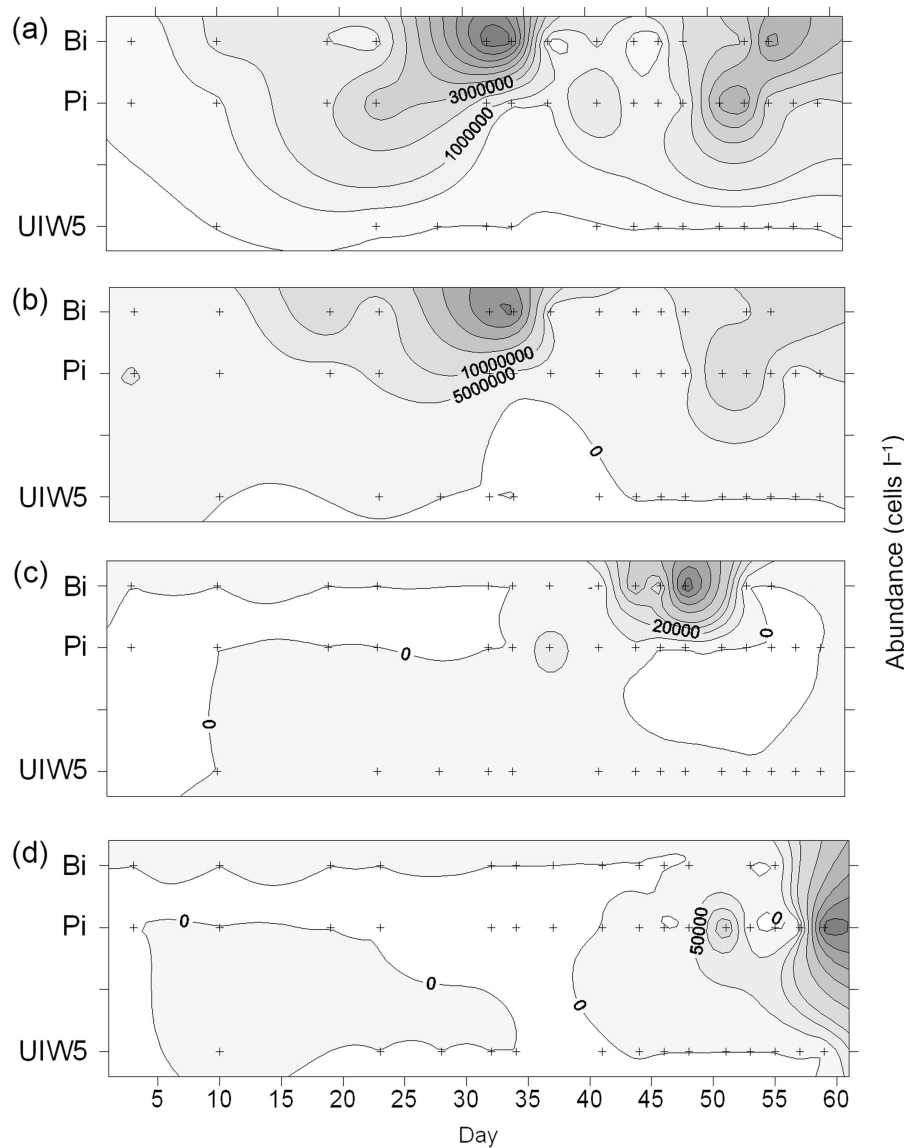


Fig. 13 Temporal variations in cell abundance for some other algal taxa (a) nanoflagellates (6–10 μm), (b) nanoflagellates (<5 μm), (c) *Gymnodinium*/*Gyrodinium* (<20 μm) and (d) *Phaeocystis antarctica* in bottom ice (Bi), platelet ice (Pi) and sub-ice water at 5-m depth (UIW5) at station R1 in Pierre Lejay Bay from 1 November (day 1) to 29 December 2001 (day 59).

effect on light availability. Ice thickness was low (60 cm) at the 1995 break-up compared to that in 2001 (101 cm). The timing of the spring break-up may also be related to the ice thickness and to biomass differences between years: the break-up occurred between 21 and 27 December in 1995 compared to 10 January 2002. The high biomass may generate heat that could accelerate the melting of the ice. The microalgal biomass increased, but irregularly, in Bi and Pi in 2001, with several peaks, especially during the last period of time series (Fig. 9b). A noticeable increase in the sub-ice irradiance at 1 m was positively related to the snow cover ablation (Fig. 5), but

with several lower records in relation to snow events. The snow cover is an important factor that decreases the light penetration to the Bi and, therefore, may influence the variations in the sympagic microalgal biomass (Arrigo et al. 1995). There are three periods showing a significant increase in Chl *a* biomass in 2001 (around day 20 and day 32 and between days 47 and 60; Fig. 5) that may be linked, with a lag of 5–10 days, to an increase in irradiance and snow cover ablation (Fig. 5). The Phaeo *a* concentrations in Bi and Pi strikingly increased towards the last 10 days of the 2001 sampling period, in parallel with a decrease of the Chl *a*:Phaeo *a* ratio (data not

Table 4 Breakdown of similarities within groups into contributions from each taxonomic entity. Taxa are ordered by decreasing average contribution (contrib.%) to a total of 90%. Average abundance (av. abund.): cells ml⁻¹.

Group Bi			
Average similarity (av. sim.): 48			
Species	Av. abund.	Av. sim.	Contrib. (%)
<i>Nitzschia stellata</i>	24 373	11	23
Nanoflagellates, ≤5 μm	12 551	9	18
<i>Navicula glaciei</i>	11 641	8	16
<i>Berkeleya adeliensis</i>	13 013	7	15
Nanoflagellates, 6–10 μm	2 682	4	7
<i>Nitzschia lecontei</i>	4 339	3	6
<i>Fragilariopsis cylindrus</i>	645	2	4
Group Pi			
Average similarity: 53			
Species	Av. abund.	Av. sim.	Contrib. (%)
<i>Nitzschia stellata</i>	12 664	10	19
<i>Navicula glaciei</i>	18 975	10	19
Nanoflagellates, ≤5 μm	5 416	10	19
<i>Berkeleya adeliensis</i>	6 795	6	11
Nanoflagellates, 6–10 μm	1 883	5	10
<i>Nitzschia lecontei</i>	4 568	5	9
<i>Fragilariopsis cylindrus</i>	374	2	4
Group UIW5			
Average similarity: 51			
Species	Av. abund.	Av. sim.	Contrib. (%)
Nanoflagellates, ≤5 μm	112	16	31
Nanoflagellates, 6–10 μm	26	8	16
<i>Navicula glaciei</i>	106	6	12
<i>Nitzschia lecontei</i>	18	4	8
<i>Gymnodinium</i>			
<i>Gyrodinium</i> , <20 μm	2	3	7
<i>Nitzschia stellata</i>	3	2	5
<i>Fragilariopsis curta</i>	2	2	4
Nanoflagellates, 11–20 μm	2	2	4
<i>Banquisia belgicae</i>	1	1	2
<i>Phaeocystis antarctica</i>	1	1	1

shown), which can be explained by a decaying Bi community and unhealthy algal cells. This is confirmed by high PO₄⁻ and NO₂⁻ concentrations in Bi and Pi at the end of the study period, which was related to remineralization of the organic material.

The high proportion of empty frustules in the sub-ice waters in 2001 may signal active sedimentation from the productive Bi and Pi horizons and a fast turnover of the microalgal organic matter through the bacterial loop or grazing long before the ice break-up (Lizotte 2003). Nevertheless, copepods and other metazoa were rare in the land-fast ice off Adélie Land (Fiala et al. 2006; G.S. Dieckmann, pers. obs.). The function of the grazing in the ice is therefore unclear. The microbial loop activity at

the sea-ice interface is also unclear since the bacterial biomass is assumed to be low in the land-fast ice off Adélie Land: bacteria and protozoa represent only 16.4 % and 3% of the total carbon microbial biomass, respectively (Delille et al. 2002).

The particle flux under the fast ice has been reported to sharply increase during a short period of two to three months in Lützow-Holm Bay (Matsuda et al. 1987; Leventer 2003). The extrapolate fast-ice flux off Adélie Land (≥7 g POC m⁻² yr⁻¹) is higher than that reported from the Weddell Sea in similar conditions (Fischer et al. 1988: 0.37 g m⁻² yr⁻¹), but lower than from Bransfield Strait or the Ross Sea (Wefer et al. 1990: 60 g m⁻² yr⁻¹; Leventer 2003). Regarding the high variability of these under-ice fluxes around Antarctica, we can note that the Pi horizon is variable in thickness and may restrict biogeochemical exchanges between the sea ice and the underlying waters (Thomas et al. 2001).

The relatively high pigment concentrations of the sedimented material at spring (as also observed in Lützow Bay by Matsuda et al. [1987]) argue for a fast downward particle flux near the coast. Nevertheless, the sub-ice “progressive vector of currents” in surface waters off the Dumont d’Urville Station, recorded for the first time in that area, supported an effective offshore export of the particulate matter. Further experiments would allow the quantification of the particulate matter potentially dispersed offshore by this drift. The preservation of microalgae and the downward fluxes to the sediment surface have been reported in other parts of Antarctica—for example, in Bransfield Strait (Kim et al. 2004) and in Lützow-Holm Bay (Tanimura et al. 1990)—and may contribute to palaeo-reconstructions (Armand & Leventer 2003; Buffen et al. 2007). Furthermore, this progressive movement of currents oriented west–northwest and the open shape of Pierre Lejay Bay would support an outflow of the ice pack after the break-up and may also partially explain why the land-fast ice is relatively thin in this part of Antarctica.

As reported in Ushio (2006) for Lützow-Holm Bay, the fast-ice break-up conditions in the Antarctic vary considerably from one year to another, and depend on oceanic and atmospheric conditions, which are rarely discussed in ecological surveys. In 2001, the ice break-up in the Pierre Lejay Bay was delayed by approximately two weeks compared to average annual data (not shown) and occurred on 10 January 2002 (day 70). Several periods with strong winds coming from the continent (up to 130 km h⁻¹) in early January 2002 (Fig. 3) may trigger some upwelling events of warmer deep waters, as suggested in Fig. 6. During this same period, a steady and significant swell along with strong

Table 5 Breakdown of dissimilarities between groups into contributions from each taxonomic entity. Taxa are ordered by decreasing average contribution (contrib. %) to a total of about 90%. Average abundance (av. abund.): cells ml⁻¹.

Groups bottom ice (Bi) and platelet ice (Pi) average dissimilarity (av. diss.) = 89				
Species	Group Bi av. abund.	Group Pi av. abund.	Av. diss.	Contrib. (%)
<i>Nitzschia stellata</i>	24 373	12 664	7	15
<i>Navicula glaciei</i>	11 641	18 975	7	15
<i>Berkeleya adeliensis</i>	13 013	6 795	6	13
Nanoflagellates, ≤5 μm	12 551	5 416	5	10
<i>Nitzschia lecointei</i>	4 339	4 568	4	9
Nanoflagellates, 6–10 μm	2 682	1 883	3	5
<i>Cylindrotheca closterium</i>	759	316	2	4
<i>Nitzschia</i> sp. 1	873	157	2	3
<i>Fragilariopsis cylindrus</i>	645	374	1	3
<i>Navicula</i> sp. 1	592	300	1	3
Protozoa sp. 1	196	267	1	2
<i>Synedropsis recta</i>	364	176	1	2
Nanoflagellates, 11–20 μm	220	240	1	2
<i>Banquisia belgicae</i>	102	65	1	1
Chrysophyceae cyst	43	90	1	1
<i>Nitzschia taeniiformis</i>	58	57	1	1

Groups Bi and UIW5 and under-ice water at 5 m (UIW5) av. diss. = 89				
Species	Group Bi av. abund.	Group UIW5 av. abund.	Av. diss.	Contrib. (%)
<i>Nitzschia stellata</i>	24 373	3	18	20
<i>Berkeleya adeliensis</i>	13 013	1	14	15
Nanoflagellates, ≤5 μm	12 551	112	12	13
<i>Navicula glaciei</i>	11 641	106	12	13
<i>Nitzschia lecointei</i>	4 339	18	6	7
Nanoflagellates, 6–10 μm	2 682	26	5	6
<i>Fragilariopsis cylindrus</i>	645	3	4	4
<i>Cylindrotheca closterium</i>	759	1	3	3
<i>Nitzschia</i> sp. 1	873	1	3	3
Nanoflagellates, 11–20 μm	220	2	2	2
<i>Synedropsis recta</i>	364	1	1	2
<i>Navicula</i> sp. 1	592	1	1	1
<i>Banquisia belgicae</i>	102	1	1	1

Groups Pi and UIW5 av. diss. = 89				
Species	Group Pi av. abund.	Group UIW5 av. abund.	Av. diss.	Contrib. (%)
<i>Navicula glaciei</i>	18 975	106	16	18
<i>Nitzschia stellata</i>	12 664	3	15	17
Nanoflagellates, ≤5 μm	5 416	11	11	12
<i>Berkeleya adeliensis</i>	6 795	1	10	12
<i>Nitzschia lecointei</i>	4 568	18	7	8
Nanoflagellates, 6–10 μm	1 883	26	6	7
<i>Fragilariopsis cylindrus</i>	374	3	3	4
Nanoflagellates, 11–20 μm	240	2	2	2
Protozoa sp. 1	267	0	2	2
<i>Synedropsis recta</i>	176	1	1	2
<i>Cylindrotheca closterium</i>	316	1	1	2
<i>Nitzschia</i> sp. 1	157	1	1	2
<i>Navicula</i> sp. 1	300	1	1	1
<i>Archaeomonas</i> cyst	90	0	1	1
Flagellate sp. 2	105	0	1	1
<i>Amphiprora kufferathii</i>	54	0	1	1

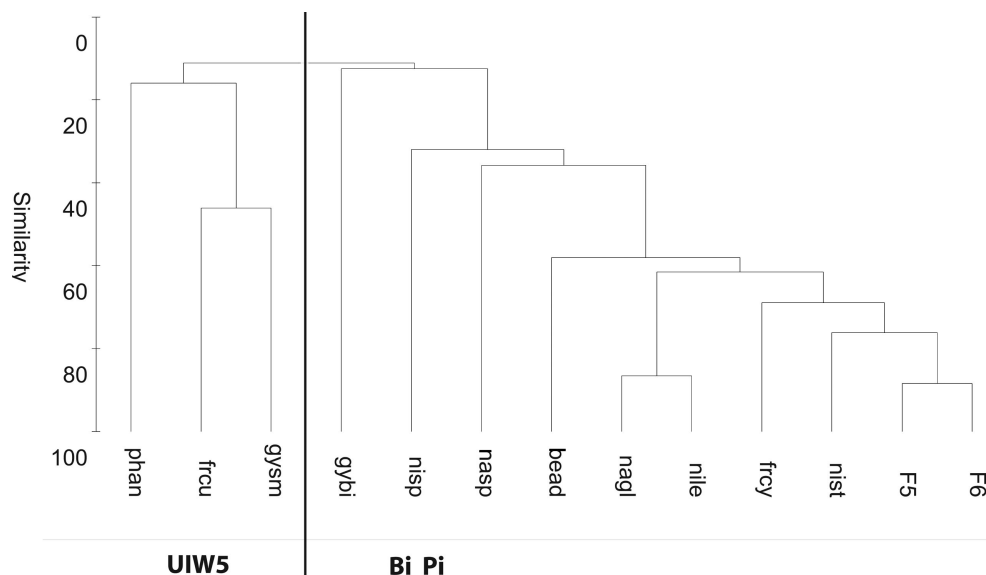


Fig. 14 Cluster using group-average linking on Bray-Curtis species (and microalgae groups) similarity from standardized abundance data. The most important species or morphotypes, with a contribution >5%, were retained from the original list. Two groups—UIW5 (sub-ice water at 5-m depth) and Bi Pi (bottom ice and platelet ice algae)—defined at an arbitrary similarity level of 12%, are indicated. Nanoflagellates less than 5 μm are denoted as F5 and those in the size range of 6–10 μm are F6. See Table 6 for the significance of the other abbreviations.

east wind contributed to the ice break-up along the coast, even if the ice was still 1 m thick. The effective ice break-up at the coast on Pierre Lejay Bay occurred one month after the end of the study reported in this article. However, the pack ice was breaking up 100–150 km offshore some weeks before the experiment, as observed on satellite imagery (Fig. 2) and as generally observed at that period of the year in the area of the station (Riaux-Gobin et al. 2005).

Taxonomic succession

As reported by Krebs et al. (1987) and Lizotte (2001), the temporal variation in species composition of first-year land-fast ice and whether these changes are related to sea-ice ecology are scarce for the Antarctic (Cota & Sullivan 1990; Watanabe et al. 1990; Gleitz et al. 1998). Moline & Prézelin (1996) reported factors regulating the variability in coastal Antarctic phytoplankton and they stated that the changes in phytoplankton successional patterns may be a more sensitive marker of detecting long-term trends in Southern Ocean ecosystems than biomass or productivity indices. The succession of sympagic microalgae may be a good marker of environmental sea-ice changes, while the microalgal biomass is variable from one year to another, as reported in this study. The 2001 sympagic microalgal time succession was the first to be analysed and illustrated for the Dumont d'Urville area. Drawing from results of previous studies at the same

sampling site, we can point out that the dominant species were the same (Riaux-Gobin et al. 2005). Nevertheless, in 1995 (Riaux-Gobin et al. 2005) the colonization of the different ice horizons may have been slightly different, with the Pi more deeply colonized than in 2001 when the Pi was enriched in microalgae only at the end of the sampling period. It would be of interest to study other time series in the same area, with comparable environmental conditions, to arrive at a conclusion regarding the reproducibility of the taxa succession.

In 2001, a succession took place with some taxa appearing late in the season such as *Berkeleya adeliensis* and *Phaeocystis antarctica* (Figs. 12, 13). Some taxonomic differences appeared between the Bi and Pi horizons throughout the sampling period (Tables 4, 5, Figs. 11–13). For example, *Fragilariopsis cylindrus* and *Nitzschia stellata* were mostly associated with the Bi while *Amphiprora kufferathii* and *Navicula glaciei* mainly occurred in the Pi. These observations support the hypothesis about the different origin—history and way of formation—of the Bi and Pi layers, as first reported by Riaux-Gobin et al. (2000). Similar taxonomic differences between Bi and Pi were also recorded in the Weddell Sea by Günther & Dieckmann (2001). Some species switched over time from the Bi to the Pi, such as *Berkeleya adeliensis*, *Fragilariopsis curta*, *F. cylindrus* and *Nitzschia lecontei*. The opportunistic tube-dwelling sea-ice diatom *B. adeliensis* is apparently well adapted to changes in texture during ice melting, while other diatoms died or were flushed from

Table 6 Bottom ice spatial heterogeneity test at R1 in Pierre Lejay Bay in 1999 (unpubl. data), along a “Latin square” (625 m²), with duplicates at 3-m intervals at each of the five “Latin square” sites. Each coring site is defined by its position (in metres).

	X (m)	Y (m)	PO ₄ ^{-a} (μM)	Si(OH) ₄ ^b (μM)	NO ₃ ^{-c} (μM)	Chl <i>a</i> ^d (μg l ⁻¹)	Phaeo <i>a</i> ^e (μg l ⁻¹)	Ice core (cm)	Snow (cm)
	1.00	-26.00	6.2	20.2	17.9	900	0.61	121.00	1.50
	4.00	-26.00	9.4	14.6	27.8	870	0.37	121.00	1.50
Mean			7.8	17.4	22.9	885	0.49	121.00	1.50
SD ^f			2.2	4.0	6.9	21	0.17	0.00	0.00
	26.00	-26.00	4.8	10.7	38.0	435	0.62	116.45	8.00
	29.00	-26.00	6.3	17.7	26.8	338	0.98	119.00	22.00
Mean			5.6	14.2	32.4	387	0.80	117.73	15.00
SD			1.1	4.9	7.9	69	0.26	1.80	9.90
	26.00	-1.00	5.4	16.4	15.5	240	0.68	112.50	24.00
	29.00	-1.00	6.3	15.3	16.9	268	0.31	109.50	25.00
Mean			5.8	15.8	16.2	254	0.49	111.00	24.50
SD			0.6	0.8	0.9	20	0.26	2.12	0.71
	1.00	-1.00	7.1	12.9	19.2	1071	0.82	124.50	2.50
	4.00	-1.00	8.5	16.9	14.1	770	0.68	122.50	2.00
Mean			7.8	14.9	16.7	921	0.75	123.50	2.25
SD			0.9	2.8	3.6	213	0.10	1.41	0.35
	13.50	-13.50	8.1	13.0	25.4	707	0.62	123.50	2.00
	16.50	-13.50	3.8	23.5	1.9	421	0.79	123.00	25.00
Mean			6.0	18.2	13.6	564	0.70	123.25	13.50
SD			3.0	7.4	16.6	202	0.12	0.35	16.26
Total mean			6.6	16.1	20.3	602	0.65	119.29	11.35
SD			1.7	3.7	9.7	297	0.20	4.95	11.08

^aPhosphate.

^bSilicic acid.

^cNitrate.

^dChlorophyll *a*.

^ePhaeopigment *a*.

^fStandard deviation.

the Bi to the Pi and the water column, probably due to the physical changes occurring in the melting ice. An increase in *B. adeliensis* during melting was also noticed in 1995 off Adélie Land (Riaux-Gobin & Poulin 2004). This Antarctic ice diatom is known to form tubular colonies creating mats or hanging strands underneath the bottom part of the ice (Hoshiai 1977; Sasaki & Hoshiai 1986; Watanabe 1988; McMinn et al. 2000).

Amphiprora kufferathii, nearly absent at the end of the present time series, was also noticed to decrease in late December in the Bi near Syowa Station, whereas *Nitzschia stellata* was increasing concurrently (Watanabe et al. 1990). Archer et al. (1996), describing a fast-ice community near Davis Station, showed the decay of autotrophic diatoms such as *Entomoneis Ehrenberg*, followed by an increase in heterotrophic organisms (i.e., euglenoids and dinoflagellates). In the present study, nanoflagellates and small gymnodinioid cells also appeared in the Bi after the disappearance of *A. kufferathii*, *Navicula glaciei* and *Nitzschia lecointei*.

The last weeks before the ice break-up are characterized by: (1) a higher under-ice irradiance that triggers a sympagic production; (2) the ice melt, promoting the growth of flagellates and particularly prymnesiophytes; and (3) a peak of degraded pigments and the decay of a large part of the colonial pennate diatom community such as *Amphiprora kufferathii* or *Berkeleya adeliensis* that form macroscopic clumps, noticed loosely attached to the bottom of the Bi at the end of the time series.

Conclusion

The 2001 short time series at R1 in Pierre Lejay Bay, near the Dumont d'Urville Station, helped to discriminate differences in colonization and the spring succession in the sympagic community between the Bi and Pi horizons. The sediment trap experiment provided a valuable indication of biomass (biological flux) released by the sea ice just before the ice break-up, and thereby may document the biological pump (Honjo 2004). Surprisingly, the Chl *a*:Phaeo *a* ratio was very high in this material, and may prove that the sedimentation was fast. During the last month before the ice break-up, the sympagic community was dominated by the tube-dwelling *Berkeleya adeliensis* that formed macroscopic aggregates and clumps at the ice–water interface; these aggregates may sediment rapidly and reach the benthos without appreciable grazing. A survey of the coast to offshore variation in particle fluxes and a survey of the metazoa present under the land-fast ice (secondary production) would complete that first study, and provide a more reliable basis for models. As a first indication,

during a 2007 cruise on the same area, we had the opportunity to do ROV surveys near our R1 site and no krill was detected (G.S. Dieckmann, pers. obs.).

The sympagic community exhibited short-term and rapid succession before the ice break-up and a movement from Bi to Pi and below. This shift of sympagic microalgae from fast ice to the underlying water masses generates a particle flux, starting long before the ice break-up in that part of Antarctica.

Acknowledgements

The authors thank the over-wintering team members for their field assistance and fellowship during EPONTA programmes, and the crew of the icebreaker *Astrolabe*. Many thanks are also due to the Météo France meteorological team at the Dumont d'Urville Station, particularly Raymond Beugin and Geneviève Caisso. They also thank Francis Gallois (Centre de Nouméa, Research Institute for Development, Nouméa, France), Louise Oriol and Jocelyne Caparros (Banyuls-sur-Mer Biological Oceanography Laboratory), Jean-Claude Duchêne (Unité Mixte de Recherche, Environnements et Paléoenvironnements Océaniques et Continentaux, Bordeaux, France) and Mélanie Simard (Institut des sciences de la mer de Rimouski, L'Université du Québec à Rimouski) for their collaboration. They thank two anonymous reviewers for their helpful comments. Sediment traps were provided by the Alfred Wegener Institute (Bremerhaven, Germany). M.P. acknowledges the Natural Sciences and Engineering Research Council of Canada and the Canadian Museum of Nature for research grants. Funds and logistic assistance in the field were supported by the French Polar Institute Paul Emile Victor.

References

- Archer S.D., Leakey R.J.G., Burkill P.H., Sleigh M.A. & Appleby C.J. 1996. Microbial ecology of sea ice at a coastal Antarctic site: community composition, biomass and temporal change. *Marine Ecology Progress Series* 135, 179–195.
- Armand L.K. & Leventer A. 2003. Palaeo sea ice distribution—reconstruction and palaeoclimatic significance. In D.N. Thomas & G.S. Dieckmann (eds.): *Sea ice. An introduction to its physics, chemistry, biology and geology*. Pp. 333–372. Oxford: Blackwell Science.
- Arrigo K., Dieckmann G., Gosselin M., Robinson D.H., Fritsen C.H. & Sullivan C.W. 1995. High resolution study of the platelet ice ecosystem in McMurdo Sound, Antarctica biomass, nutrient, and production profiles within a dense microalgal bloom. *Marine Ecology Progress Series* 127, 255–268.

- Arrigo K. & Thomas D.N. 2004. Large scale importance of sea ice biology in the Southern Ocean. *Antarctic Science* 16, 471–486.
- Bray J.R. & Curtis J.T. 1957. An ordination of the upland forest communities of southern Wisconsin. *Ecological Monographs* 27, 325–349.
- Buffen A., Leventer A., Rubin A. & Hutchins T. 2007. Diatom assemblages in surface sediments of the northwestern Weddell Sea, Antarctic Peninsula. *Marine Micropaleontology* 62, 7–30.
- Clarke K.R. & Warwick R.M. 2001. A further biodiversity index applicable to species lists: variation in taxonomic distinctness. *Marine Ecology Progress Series* 216, 265–278.
- Comiso J.C. 2003. Large-scale characteristics and variability of the global sea ice cover. In D.N. Thomas & G.S. Dieckmann (eds.): *Sea ice. An introduction to its physics, chemistry, biology and geology*. Pp. 112–142. Oxford: Blackwell Science.
- Cota G.F. & Sullivan C.W. 1990. Photoadaptation, growth and production of bottom ice algae in the Antarctic. *Journal of Phycology* 26, 399–411.
- Delille D., Fiala M., Kuparinen J., Kuosa H. & Plessis C. 2002. Seasonal changes in microbial biomass in the first-year ice of the Terre Adélie area (Antarctica). *Aquatic Microbial Ecology* 28, 257–265.
- Dieckmann G., Rohardt G., Hellmer H. & Kipfstuhl J. 1986. The occurrence of ice platelets at 250 m depth near the Filchner Ice Shelf and its significance for sea ice biology. *Deep-Sea Research* 33, 141–148.
- Fiala M., Kuosa H., Kopczynska E.E., Oriol L. & Delille D. 2006. Spatial and seasonal heterogeneity of sea ice microbial communities in the first-year ice of Terre Adélie area (Antarctica). *Aquatic Microbial Ecology* 43, 95–106.
- Fischer G., Fuetterer D., Gersonde R., Honjo S., Ostermann D.R. & Wefer G. 1988. Seasonal variability of particle flux in the Weddell Sea and its relation to ice cover. *Nature* 335, 426–428.
- Foldvik A. & Kvinge T. 1977. Thermohaline convection in the vicinity of an ice shelf. In M.F. Dunbar (ed.): *Polar oceans: proceedings of the Polar Oceans Conference*. McGill University, Montreal, May 1974. Pp. 247–255. Calgary: Arctic Institute of North America.
- Fonda Umani S., Monti M., Bergamasco A., Cabrini M., De Vittor C., Burba N. & Del Negro P. 2005. Plankton community structure and dynamics versus physical structure from Terra Nova Bay to Ross Ice Shelf (Antarctica). *Journal of Marine Systems* 55, 31–46.
- Garrison D.L. & Buck K.R. 1989. The biota of Antarctic pack ice in the Weddell Sea and Antarctic Peninsula regions. *Polar Biology* 10, 211–219.
- Garrity C., Ramseier R.O., Peinert R., Kern S. & Fischer G. 2005. Water column particulate organic carbon modeled fluxes in the ice-frequented Southern Ocean. *Journal of Marine Systems* 56, 133–149.
- Gleitz M., Bartsch A., Dieckmann G. & Eicken H. 1998. Composition and succession of sea ice diatom assemblages in the eastern and southern Weddell Sea, Antarctica. *Antarctic Research Series* 73, 107–120.
- Guglielmo L., Carrada G.C., Catalano G., Cozzi S., Dell'Anno A., Fabiano M., Granata A., Lazzara L., Lorenzelli R., Manganaro A., Mangoni O., Mistic C., Modigh M., Pusceddu A. & Saggiomo V. 2004. Biogeochemistry and algal communities in the annual sea ice at Terra Nova Bay (Ross Sea, Antarctica). *Chemistry and Ecology* 20 (Supplement 1), 43–55.
- Günther S. & Dieckmann G. 2001. Vertical zonation and community transition of sea-ice diatoms in fast ice and platelet layer, Weddell Sea, Antarctica. *Annals of Glaciology* 33, 287–296.
- Günther S., Gleitz M. & Dieckmann G. 1999. Biogeochemistry of Antarctic sea ice: a case study on platelet ice layers at Drescher Inlet, Weddell Sea. *Marine Ecology Progress Series* 177, 1–13.
- Hasle G.R., Medlin L.K. & Syvertsen E.E. 1994. *Synedropsis* gen. nov., a genus of araphid diatoms associated with sea ice. *Phycologia* 33, 248–270.
- Hasle G.R. & Syvertsen E.E. 1996. Marine diatoms. In C.R. Tomas (ed.): *Identifying marine diatoms and dinoflagellates*. Pp. 387–584. San Diego: Academic Press.
- Honjo S. 2004. Particle export and biological pump in the Southern Ocean. *Antarctic Science* 16, 501–516.
- Hoshiai T. 1977. Seasonal change of ice communities in the sea ice near Syowa Station, Antarctica. In M.J. Dunbar (ed.): *Polar oceans*. Pp. 307–317. Calgary: Arctic Institute of North America.
- Jacobs S. 2006. The determination of nitrogen in biological materials. In D. Glick (ed.): *Methods of biochemical analysis Vol. 13*. Pp. 241–263. Hoboken: John Wiley & Sons.
- Kim D., Kim D.-Y., Kim Y.-J., Kang Y.-C. & Shim J. 2004. Downward fluxes of biogenic material in Bransfield Strait, Antarctica. *Antarctic Science* 16, 227–237.
- Krebs W.N., Lipps J.H. & Burckle L.H. 1987. Ice diatom flora, Arthur Harbor, Antarctica. *Polar Biology* 7, 163–171.
- Leonard G.H., Purdie C.R., Langhorne P.J., Haskell T.G., Williams M.J.M. & Frew R.D. 2006. Observations of platelet ice growth and oceanographic conditions during the winter of 2003 in McMurdo Sound, Antarctica. *Journal of Geophysical Research—Space Physics* 111, C04012, doi: 10.1029/2005JC002952.
- Le Roy R. & Simon B. 2003. *Réalisation et validation d'un modèle de marée en Manche et dans le golfe de Gascogne. Application à la réalisation d'un nouveau programme de réduction des sondages bathymétriques. (Creation and validation of a tidal model in the English Channel and the Gulf of Gascogne. Implementation for a new programme to reduce bathymetric surveys.) Rapport SHOM 002/03*. Brest: Service Hydrographique et Océanographique de la Marine.
- Leventer A. 2003. Particulate flux from sea ice in polar waters. In N. David et al. (eds.): *Sea ice. An introduction to its physics, chemistry, biology and geology*. Pp. 303–332. Oxford: Blackwell Science.
- Leventer A. & Dunbar R.B. 1987. Diatom flux in McMurdo Sound, Antarctica. *Marine Micropaleontology* 12, 49–64.
- Lizotte M.P. 2001. The contributions of sea ice algae to Antarctic marine primary production. *American Zoologist* 41, 57–73.

- Lizotte M.P. 2003. The microbiology of sea ice. In N. David et al. (eds.): *Sea ice. An introduction to its physics, chemistry, biology and geology*. Pp. 184–210. Oxford: Blackwell Science.
- Lund J.W.G., Kipling C. & LeCren E.D. 1958. The inverted microscope method of estimating algal numbers and the statistical basis of estimations by counting. *Hydrobiologia* 11, 143–170.
- Manguin E. 1957. Premier inventaire des diatomées de la Terre Adélie Antarctique: espèces nouvelles. (The first diatom survey from Adélie Land, Antarctica: new species.) *Revue Algologique Nouvelle Série* 3, 111–134.
- Manguin E. 1960. Les diatomées de la Terre Adélie, campagne du "Commandant Charcot" 1949–1950. (Diatoms from Adélie Land, the «Commandant Charcot» 1949–1950 expedition). *Annales des Sciences Naturelles-Botanique et Biologie Végétale* 1, 223–363.
- Matsuda O., Ishikawa S. & Kawaguchi K. 1987. Seasonal variation of downward flux of particulate organic matter under the Antarctic fast ice. *Proceedings of the NIPR Symposium on Polar Biology* 1, 23–34.
- McMinn A. 1996. Preliminary investigation of the contribution of fast-ice algae to the spring phytoplankton bloom in Ellis Fjord, eastern Antarctica. *Polar Biology* 16, 301–307.
- McMinn A., Ashworth C. & Ryan K. 2000. In situ net primary productivity of an Antarctic fast ice bottom algal community. *Aquatic Microbial Ecology* 21, 177–185.
- McMinn A., Ryan K.G., Ralph P. & Pankowski A. 2007. Spring sea ice photosynthesis, primary productivity and biomass distribution in eastern Antarctica, 2002–2004. *Marine Biology* 151, 985–995.
- Medlin L.K. & Priddle J. 1990. *Polar marine diatoms*. Cambridge: British Antarctic Survey.
- Moline M.A. & Prézélin B.B. 1996. Palmer LTER 1991–1994: Long-term monitoring and analyses of physical factors regulating variability in coastal Antarctic phytoplankton biomass, in situ productivity and taxonomic composition over subseasonal, seasonal and interannual time scales. *Marine Ecology Progress Series* 145, 143–160.
- Neveux J. & Lantoiné F. 1993. Spectrofluorometric assay of chlorophylls and phaeopigments using the least squares approximation technique. *Deep-Sea Research* 40, 1747–1765.
- Palmisano A.C. & Garrison D.L. 1993. Microorganisms in Antarctic sea ice. In E.I. Friedmann (ed.): *Antarctic microbiology*. Pp. 167–218. New York: Wiley-Liss.
- Parsons T.R., Maika Y. & Lalli C.M. 1984. *A manual of chemical and biological methods of seawater analysis*. Oxford: Pergamon Press.
- Pineau L. 1999. *Amélioration du modèle de prédiction de marée en Manche. (Improvement of predictive tidal models in the English Channel.) Technical Report SHOM 282 EPSHOM/CH/GG/ET/NP du 28.05.99*. Brest: Service Hydrographique et Océanographique de la Marine.
- Poulin M., Riaux-Gobin C., Compère P. & Simard M. 2006. Le genre *Entomoneis* à Terre Adélie, Antarctique. (The genus *Entomoneis* in Adélie Land, Antarctica.) *Symbioses, nouvelle série* 14, 51.
- Priddle J. & Fryxell G. 1985. *Handbook of the common plankton diatoms of the Southern Ocean: Centrales except the genus Thalassiosira*. Cambridge: Cambridge University Press.
- Redfield A.C., Ketchum B.H. & Richards F.A. 1963. The influence of organisms on the composition of sea-water. In M.N. Hill (ed.): *The sea. Vol. 2*. Pp. 26–77. New York: John Wiley & Sons.
- Riaux-Gobin C. & Poulin M. 2004. Possible symbiosis of *Berkeleya adeliensis* Medlin, *Synedropsis fragilis* (Manguin) Hasle et al. and *Nitzschia lecontei* Van Heurck (Bacillariophyta) associated with land-fast ice in Adélie Land, Antarctica. *Diatom Research* 19, 265–274.
- Riaux-Gobin C., Poulin M., Dieckmann G., Labrune C. & Vétion G. 2011. Spring phytoplankton onset after the ice break-up and sea-ice signature (Adélie Land, East Antarctica). *Polar Research* 30, 1–11.
- Riaux-Gobin C., Poulin M., Prodon R. & Tréguer P. 2003. Land-fast ice microalgal and phytoplanktonic communities (Adélie Land, Antarctica) in relation to environmental factors during ice break-up. *Antarctic Science* 15, 353–364.
- Riaux-Gobin C. & Stumm K. 2006. Modern Archaeomonadaceae from the land-fast ice off Adélie Land (Antarctica): a preliminary report. *Antarctic Science* 18, 51–60.
- Riaux-Gobin C., Tréguer P., Dieckmann G., Maria E., Vétion G. & Poulin M. 2005. Land-fast ice off Adélie Land (Antarctica): short-term variations in nutrients and chlorophyll just before ice break-up. *Journal of Marine Systems* 55, 235–248.
- Riaux-Gobin C., Tréguer P., Poulin M. & Vétion G. 2000. Nutrients, algal biomass and communities in land-fast ice and seawater off Adélie Land (Antarctica). *Antarctic Science* 12, 160–171.
- Robinson D.H., Arrigo K.R., Kolber Z., Gosselin M. & Sullivan C.W. 1998. Photophysiological evidence of nutrient limitation of platelet ice algae in McMurdo Sound, Antarctica. *Journal of Phycology* 34, 788–797.
- Sasaki H. & Hoshiai T. 1986. Sedimentation of microalgae under the Antarctic fast ice in summer. *Memoirs of the National Institute of Polar Research, Special Issue* 40, 45–55.
- Scott F.J. & Marchand H.J. 2005. *Antarctic marine protists*. Canberra: Australian Biological Resources Study/Hobart: Australian Antarctic Division.
- Tanimura Y., Fukuchi M., Watanabe K. & Moriwaki K. 1990. Diatoms in water column and sea-ice in Lützow-Holm Bay, Antarctica, and their preservation in the underlying sediments. *Bulletin of the National Science Museum, Tokyo, Series C* 16, 15–39.
- Thomas D.N., Kennedy H., Kattner G., Gerdes D., Gough C. & Dieckmann G.S. 2001. Biogeochemistry of platelet ice: its influence on particle flux under fast ice in the Weddell Sea, Antarctica. *Polar Biology* 24, 486–496.
- Tréguer P. & Le Corre P. 1975. *Manuel d'analyses automatiques des sels nutritifs dans l'eau de mer. Utilisation de l'Auto-Analyzer II Technicon. (Manual of automatic analyses of marine nutrients. Use of the Auto-Analyzer II Technicon.)* Brest: University of Western Brittany.

- Ushio S. 2006. Factors affecting fast-ice break-up frequency in Lützow-Holm Bay, Antarctica. *Annals of Glaciology* 44, 177–182.
- Watanabe K. 1988. Sub-ice microalgal strands in the Antarctic coastal fast ice area near Syowa Station. *Japanese Journal of Phycology* 36, 221–229.
- Watanabe K., Sato H. & Hoshiai T. 1990. Seasonal variation in ice algal assemblages in the fast ice near Syowa Station in 1983/84. In K.R. Kerry & G. Hempel (eds.): *Antarctic ecosystems. Ecological change and conservation*. Pp. 136–142. Berlin: Springer.
- Wefer G., Fischer G., Fütterer D.K., Gersonde R., Honjo S. & Ostermann D. 1990. Particle sedimentation and productivity in Antarctic waters of the Atlantic sector. In U. Bleil & J. Thiede (eds.): *Geological history of the polar oceans: Arctic versus Antarctic*. Pp. 363–379. Dordrecht: Kluwer.
- Zwally H.J., Comiso J.C., Parkinson C.L., Campbell W.J., Carsey F.D. & Gloersen P. 1983. *Antarctic sea ice, 1973–1976. Satellite passive wavelength observations. NASA SP-459*. Washington, DC: National Aeronautics and Space Administration.